

Plato’s Form: Toward Backdoor Defense-as-a-Service for LLMs with Prototype Representations

Chen Chen¹, Yuchen Sun², Jiaxin Gao², Yanwen Jia²

Xueluan Gong^{1*}, Qian Wang², Kwok-Yan Lam¹

¹Nanyang Technological University, ²Wuhan University

¹{chen.chen, xueluan.gong, kwokyan.lam}@ntu.edu.sg

²{yuchensun, jiaxingao, yanwenjia, qianwang}@whu.edu.cn

Abstract

Large language models (LLMs) are increasingly deployed in security-sensitive applications, yet remain vulnerable to backdoor attacks. However, existing backdoor defenses are difficult to operationalize for Backdoor Defense-as-a-Service (BDaaS), as they require unrealistic side information (e.g., downstream clean data, known triggers/targets, or task domain specifics), and lack reusable, scalable purification across diverse backdoored models. In this paper, we present PROTOPURIFY, a backdoor purification framework via parameter edits under minimal assumptions. PROTOPURIFY first builds a backdoor vector pool from clean and backdoored model pairs, aggregates vectors into candidate prototypes, and selects the most aligned candidate for the target model via similarity matching. PROTOPURIFY then identifies a boundary layer through layer-wise prototype alignment and performs targeted purification by suppressing prototype-aligned components in the affected layers, achieving fine-grained mitigation with minimal impact on benign utility. Designed as a BDaaS-ready primitive, PROTOPURIFY supports *reusability*, *customizability*, *interpretability*, and *runtime efficiency*. Experiments across various LLMs on both classification and generation tasks show that PROTOPURIFY consistently outperforms 6 representative defenses against 6 diverse attacks, including single-trigger, multi-trigger, and triggerless backdoor settings. PROTOPURIFY reduces ASR to below 10%, and even as low as 1.6% in some cases, while incurring less than a 3% drop in clean utility. PROTOPURIFY further demonstrates robustness against adaptive backdoor variants and stability on non-backdoored models.

1 Introduction

Large Language Models (LLMs), such as GPT-5 and Llama 3, have advanced rapidly and achieved state-of-the-art performance across a wide range of natural language processing

*Corresponding author

In Plato’s philosophy, a Form is an idealized concept that captures the common structure shared by many imperfect real-world examples.

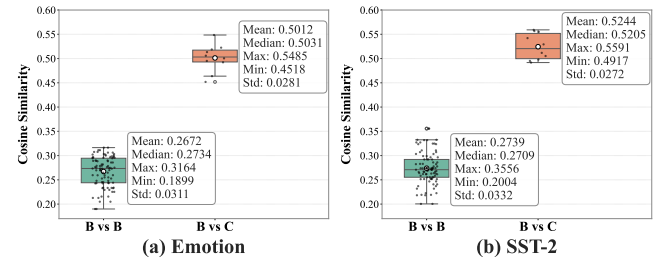


Figure 1: Cosine similarities among backdoor vectors (B vs B) and between backdoor and clean vectors (B vs C). The backdoor vectors are extracted from 5 trigger types and 4 different attacks.

(NLP) tasks [2, 53]. Their remarkable generalization capability has driven widespread adoption across diverse industries, including finance, education, and healthcare, where they are broadly deployed to automate workflows and enhance user experiences [38]. Despite these successes, LLMs remain susceptible to a variety of security threats, among which backdoor attacks pose a particularly severe risk. Backdoor attacks aim to implant malicious functionalities into the model, where an adversary may poison the training data or manipulate the model weights such that the model performs normally on benign inputs but produces predefined malicious outputs when exposed to a secret trigger [5, 55]. Detecting and mitigating such attacks is highly challenging, as triggers can take arbitrary forms, e.g., specific text strings, syntactic patterns, or visual signals, and are typically unknown to the defender. The vast scale and complex parameterization of LLMs further obscure backdoor behaviors within high-dimensional latent spaces [6, 46].

These threats motivate a managed backdoor defense service for LLMs (*Backdoor Defense-as-a-Service*, BDaaS), where model owners submit potentially compromised models for post-hoc mitigation prior to deployment. This service-oriented setting aligns with emerging commercial GenAI security offerings that provide centralized model risk assessment,

Table 1: A comparison of studies on backdoor defense approaches.

Purification method	Agnosticism [†]			Backdoor Defense-as-a-Service (BDaaS)			
	Target dataset	Target output	Target domain	Reusability*	Customizability [§]	Interpretability [‡]	Runtime efficiency [¶]
Fine-tuning [37]	X (F)	✓	X	□	□	□	□
Fine-pruning [31]	X (F)	✓	X	■	□	□	□
BadAct [51]	X (P)	✓	X	□	□	□	■
W2SDefense [57]	X (F)	✓	X	□	□	□	□
LETHE [4]	X (F)	✓	X	□	□	□	□
Obliviate [23]	X (F)	✓	X	□	□	□	□
PURE [58]	X (P)	✓	X	□	□	□	■
BTU [22]	X (F&P)	✓	X	□	□	■	□
ROME [32]	X (E)	✓	X	□	□	□	■
NAD [29]	X (P)	✓	X	□	□	□	□
SANDE [26]	✓	X	X	□	□	□	□
BEEAR [52]	✓	X	X	□	□	□	□
LMSanitizer [42]	✓	✓	X	□	□	□	■
CROW [34]	✓	✓	✓	□	□	□	□
PROTOPURIFY	✓	✓	✓	■	■	■	■

[†] **Agnosticism:** Whether the threat model lacks specific knowledge. Target dataset: downstream clean data (used for F = Finetuning, P = Probing, E = Editing). Target output: the compromised output features, such as toxicity or sentiment bias. Target domain: downstream task domain, i.e., classification or generation.

^{*} **Reusability:** How auxiliary modules or purified models can be reused for other backdoored models. □ = cannot reuse; ■ = requires adaptation; ■ = can reuse.

[§] **Customizability:** How the purification can be tailored to known types of attacks or tasks for better performance. □ = not customizable; ■ = customizable.

[‡] **Interpretability:** How the purification method can reveal the mechanisms of backdoor behaviors. □ = cannot reveal; ■ = partially reveal; ■ = fully reveal.

[¶] **Runtime efficiency:** How the purification method affects the per-model runtime efficiency. □ = needs per-model gradient-based training/optimization (e.g., fine-tuning, unlearning, distillation, or other optimization); ■ = training-free, purification via one-shot editing/pruning or a few forward-pass computations.

red-teaming, and safety scanning as a productized workflow (e.g., TrojAI Detect¹, and CalypsoAI²). However, directly deploying existing defenses in such a high-throughput service still faces substantial limitations, as summarized in Table 1. First, many approaches rely on strong assumptions. For instance, some assume access to a representative **clean target dataset** for the model’s downstream tasks, or prior knowledge of the specific **target outputs** (e.g., toxic or biased responses) activated by backdoor triggers. Others require information about the **target task domain** where the model is intended to operate (e.g., classification or generation). These assumptions are often unrealistic, as LLMs are typically designed for general-purpose applications, and such information is either unavailable or sensitive, particularly for BDaaS. Second, most existing defenses are designed to purify each compromised model independently, with no mechanism to transfer insights or components from previous efforts. This limits efficiency and scalability for service-level purification. We therefore identify four desiderata for practical backdoor purification from the literature [25], which existing methods rarely satisfy: **Reusability**, enabling defensive modules to be leveraged across diverse backdoors; **Customizability**, permitting targeted adaptation when partial information about the backdoor is available; **Interpretability**, providing transparency into how backdoors are identified or mitigated; and **Runtime efficiency**, ensuring minimal per-model runtime overhead.

In this work, we propose PROTOPURIFY, a novel backdoor mitigation method that operates under minimal assumptions about the data and downstream tasks, while inherently sup-

porting the four key desiderata. PROTOPURIFY is motivated by the observation that different backdoor attacks often induce correlated parameter shifts (Figure 1), implying a shared malicious backdoor “prototype”. PROTOPURIFY aims to identify and exploit this prototype for cross-data and cross-task backdoor mitigation. To this end, PROTOPURIFY is designed to address the following challenges:

C1. How to effectively capture backdoor behaviors in LLMs’ parameter space?

To capture backdoor behaviors in the parameter space, we adopt a weight-difference formulation that removes task-specific learning signals from malicious updates. Specifically, we simulate diverse backdoor scenarios by training paired models from the same base model under identical optimization settings: one exposed to a backdoor attack and the other trained on clean data only. We obtain a backdoor vector by computing the difference between the parameters of these two models. Applying this process across multiple datasets and attack strategies yields a collection of vectors that encode diverse backdoor behaviors.

C2. How to build a backdoor prototype vector based on the backdoor vectors?

Given the collection of backdoor vectors extracted from diverse simulated attacks, we aim to distill their shared malicious features into multiple prototype representations. To this end, we construct backdoor vectors using aggregation operations, such as Arithmetic Mean (AM) or Principal Component Analysis (PCA). These backdoor prototype vectors are designed to serve as a transferable and compact representation of backdoor features. For a target backdoored model, we then identify the most appropriate prototype via similarity

¹<https://troj.ai/products/detect>

²<https://calypsoai.com/inference-platform/>

matching and use it as the basis for model purification.

C3. How to detect the layers that encode backdoors?

We observe that overly aggressive purification can lead to a noticeable degradation in model utility. To mitigate this issue, we introduce a candidate layer detection mechanism. We first decompose both the target backdoor model’s weight update and the identified prototype vector by layers, and compute alignment scores using cosine similarity. Empirically, we find these scores are relatively stable in lower layers but exhibit a pronounced increase at deeper layers. Based on this observation, we define a boundary layer using both *Magnitude Significance* and *Increment Significance* criteria. This boundary partitions the model into protected lower layers and candidate upper layers for purification.

C4. How to purify the target backdoor model based on the prototype vector?

For each weight matrix in the target backdoor model, we obtain its update vector and decompose it into a set of independent components via matrix decomposition. By measuring the projection of each component to the prototype vector, we can identify those that are strongly associated with backdoor behavior. We then introduce a purification strength that suppresses prototype-aligned components through calibrated scaling. This design enables a controllable trade-off between the strength of the purification and its impact on model utility.

Compared with 6 state-of-the-art baseline defenses, PROTOPURIFY consistently achieves a superior mitigation-utility trade-off across diverse models, tasks, and backdoor settings. PROTOPURIFY reduces ASR from nearly 100% to below 10% while preserving high CDA on both classification and generation tasks. Extensive evaluation on 6 representative backdoor attacks demonstrates that PROTOPURIFY is effective under single-trigger, multi-trigger, and triggerless settings. Moreover, PROTOPURIFY remains robust against defense-aware adaptive adversaries and stable on non-backdoored models.

To conclude, we make the following contributions:

- We propose PROTOPURIFY, a prototype-based backdoor purification method toward Backdoor Defense-as-a-Service. It operates under minimal assumptions about triggers, training data, or downstream tasks, and is explicitly designed to satisfy *reusability*, *customizability*, *interpretability*, and *runtime efficiency* for high-throughput deployment.
- We develop an end-to-end weight-space purification pipeline that includes backdoor vector extraction via paired model simulation, prototype construction through aggregation, boundary layer detection using layer-wise alignment analysis, and controllable model purification by suppressing prototype-aligned components.
- Extensive experiments on various LLMs across both classification and generation tasks show that PROTOPURIFY consistently outperforms 6 representative defenses, achieving a superior mitigation-utility trade-off across single-trigger,

multi-trigger, and triggerless backdoors. PROTOPURIFY is also robust to adaptive backdoor attacks and stable on non-backdoored models.

2 Background

2.1 Large Language Models (LLMs)

Large Language Models (LLMs) are deep learning models designed to process and generate human-like text. Built on the Transformer architecture, they leverage self-attention mechanisms to capture complex dependencies within sequences. Prominent examples like GPT-3, GPT-4, and LLaMA have shown exceptional performance in tasks such as text generation, translation, and dialogue systems.

The training of LLMs typically involves two stages: pre-training and fine-tuning. During pre-training, the model learns a general representation of language by predicting the next token in a sequence using causal language modeling, where the objective is:

$$L_{\text{causal}} = - \sum_{i=1}^N \log P(x_i | x_{<i}; \theta) \quad (1)$$

where x_i represents the i -th token, $x_{<i}$ denotes the preceding tokens, and θ are the model parameters. The pre-training process relies heavily on the self-attention mechanism, which efficiently captures token relationships:

$$\text{Attention}(Q, K, V) = \text{softmax} \left(\frac{QK^T}{\sqrt{d_k}} \right) V \quad (2)$$

where Q , K , and V are the query, key, and value matrices, and d_k is the dimension of the key vectors.

During fine-tuning, the pre-trained model is adapted to specific downstream tasks by optimizing a task-specific loss function, such as cross-entropy. Additionally, advanced methods like *Reinforcement Learning from Human Feedback* (RLHF) are employed to align the model’s outputs with human preferences. RLHF enhances fine-tuning by introducing a reward signal derived from human evaluations, refining the model’s performance in tasks such as dialogue systems and content generation. Together, these stages enable LLMs to generalize effectively while catering to specific applications.

Despite these advancements, LLMs remain vulnerable to security threats, such as backdoor attacks and adversarial manipulations. Our work aims to address these challenges by developing robust defense mechanisms for safe deployment.

2.2 Backdoor Attacks and Defenses

Backdoor Attacks. Backdoor attacks are an insidious training-time threat where an adversary implants a hidden “trigger” pattern that causes the model to produce malicious outputs for trigger-embedded inputs, while behaving normally

on clean inputs [9, 10, 12]. With LLMs’ broad deployment and data-hungry training pipelines, backdoors become an especially serious security concern [45, 49, 50, 56]. Existing attacks are commonly categorized by trigger design into *single-trigger*, *multi-trigger*, and *triggerless* backdoors.

Single-trigger backdoor attacks use a single fixed trigger (e.g., a specific token sequence or textual pattern) to manipulate the model output. For example, Kurita et al. [24] presented a clean-label backdoor attack against BERT, where fine-tuning with a rare trigger token induces an attacker-chosen token prediction. Beyond data poisoning, BadEdit [28] demonstrated that a single-trigger backdoor can also be planted via model editing, directly modifying model weights to associate a trigger with a target behavior. However, these single-trigger designs rely on explicit lexical cues (often rare or out-of-context), which can be detected and filtered by simple outlier-word inspection defenses [36]. To improve stealth, triggers can be defined over latent linguistic features. Qi et al. [36] used a pre-specified syntactic template as the trigger, yielding fluent poisoned inputs and resisting simple token-filtering defenses, but such feature-space triggers often require controlled rewriting and may incur additional attack complexity.

Multi-trigger backdoor attacks distribute the trigger into multiple components to improve stealth and control, activating the payload only when all triggers co-occur. For example, Huang et al. [19] proposed Composite Backdoor Attack (CBA), which scatters triggers across different prompt segments (e.g., user query vs. system instruction), making accidental activation by benign inputs much less likely. Another variant is layered (dual) triggers that combine multiple linguistic features. Hou et al. [16] proposed a dual-trigger textual backdoor that is activated when two cues co-occur, namely a specific syntactic template and a subjunctive mood pattern, thereby enhancing stealth compared to token-based triggers.

Triggerless backdoor attacks remove the reliance on an explicit trigger string and instead activate the malicious behavior under covert conditions embedded in seemingly benign inputs [8, 35]. Concretely, the backdoor may be triggered at the semantic level, where a particular meaning, intent, or topic implicitly serves as the trigger, or at the syntactic level, where specific structural patterns act as hidden triggers [54]. Yan et al. [47] proposed Virtual Prompt Injection (VPI) for instruction-tuned LLMs, where a semantic trigger (e.g., a specific entity or topic) makes the model behave as if an attacker-chosen virtual prompt were implicitly appended, steering outputs without any explicit trigger string. Hao et al. [14] studied multi-turn chat models and proposed a distributed-trigger backdoor (DTBA), where scenario-level triggers are split across dialogue turns (e.g., a benign discussion together with a malicious request).

Backdoor Defenses. Backdoor defenses generally fall into two lines: detection and purification. Detection aims to flag backdoored models or triggered inputs, but it cannot restore the model to a safely deployable state. In contrast, purifi-

cation explicitly neutralizes backdoor behaviors while preserving benign utility. In this paper, we focus on backdoor purification, which can be categorized into: (1) fine-tuning based, (2) pruning-based, (3) parameter-editing based, and (4) embedding-based approaches.

Fine-tuning-based defenses purify a backdoored LLM by training on benign data to suppress malicious behaviors while preserving clean utility. However, these retraining methods are often computationally expensive and can be ineffective against advanced backdoors [27]. To address these limitations, several methods enhance fine-tuning with additional supervision or regularization. NAD [29] adopts a distillation-guided fine-tuning strategy, where a clean teacher guides the backdoored student to match intermediate-layer representations (e.g., attention) on clean data. W2SDefense [57] further improves efficiency by training a small clean teacher and distilling it into the poisoned student via parameter-efficient fine-tuning (e.g., LoRA), enabling effective backdoor unlearning without full retraining.

Pruning-based defenses purify a backdoored LLM by pruning or masking a small subset of components (e.g., neurons or attention heads) that encode backdoor behaviors, while leaving the remaining parameters unchanged. For example, Fine-Pruning [31] removes neurons with low activation on clean inputs (followed by light fine-tuning), aiming to eliminate backdoor-related units with minimal utility loss. Recently, more targeted pruning strategies have also been explored in LLMs. PURE [58] prunes backdoor-related attention heads and normalizes attention activations to suppress malicious behaviors in pre-trained language models. Obliviate [23] targets the PEFT setting, where backdoors are embedded in learned adapter modules (e.g., LoRA). It detects suspicious adapter dimensions via clean-probe statistics and then neutralizes the backdoor by selectively zeroing/re-initializing the identified adapter parameters, while keeping the frozen backbone intact. Finally, Wanda [40], originally proposed for training-free LLM pruning, can be repurposed as a lightweight purification baseline by pruning weights with small activation-aware scores $|w| \cdot |a|$, where w is a weight and a is its input activation estimated on a small set of benign calibration prompts.

Parameter-editing-based defenses treat backdoors as localized associations embedded in model weights and remove them by directly modifying a small subset of parameters, rather than retraining or pruning the model. A representative editing primitive is ROME [32], which rewrites a localized association via a low-rank update to an MLP layer. When repurposed for backdoor purification, ROME can remove a backdoor if the defender can provide explicit counterfactual pairs (triggered behavior \rightarrow desired benign behavior). Later, MEMIT [33] generalizes this paradigm to efficiently rewrite many associations at scale. Such surgical rewriting incurs no inference overhead, but assumes the triggered misbehavior can be identified and that the backdoor is sufficiently localized, limiting its effectiveness for unknown, distributed, or

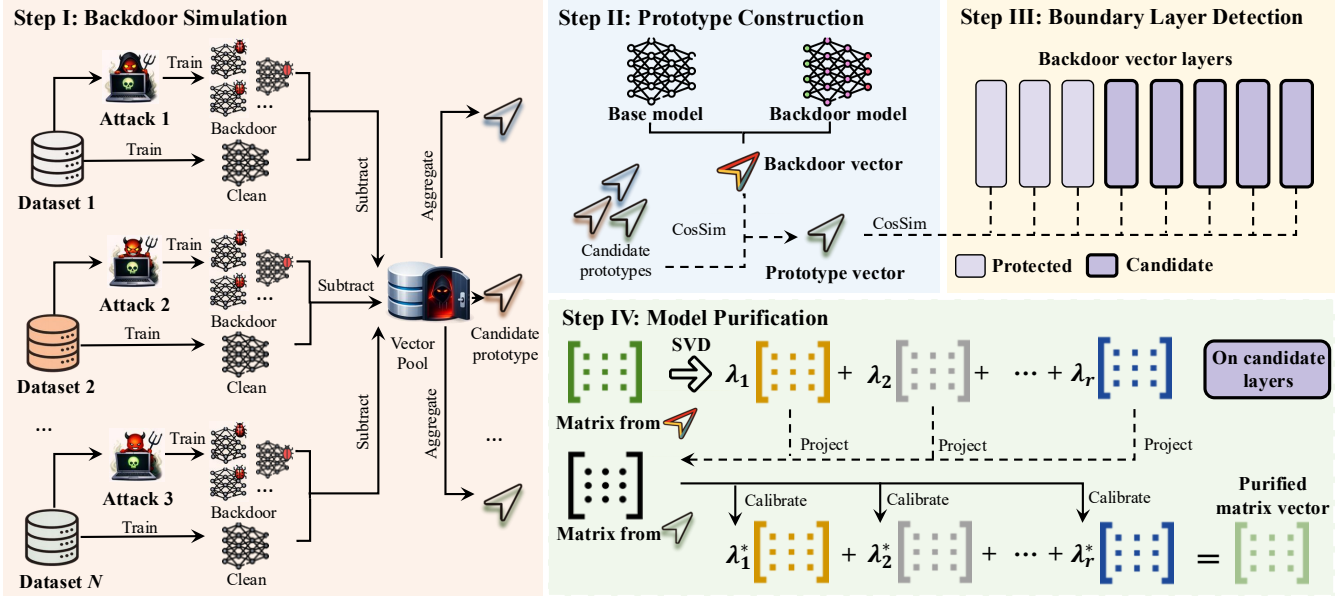


Figure 2: An overview of PROTOPURIFY. In Stage I, we simulate diverse backdoor scenarios to extract backdoor vectors from clean vs. backdoored model weights. These vectors are aggregated into prototype vectors, from which the most aligned prototype is selected for the target backdoor model in Stage II. Stage III aims to detect a boundary layer via layer-wise prototype alignment. In Stage IV, we purify candidate layers by suppressing prototype-aligned components for each matrix.

semantic triggers.

Embedding-based defenses mitigate backdoors by operating in the representation space, rather than directly modifying model weights. The core intuition is that backdoor behaviors manifest as abnormal directions in embedding space (e.g., hidden states or output representations). BEEAR [52] identifies and removes safety backdoors in instruction-tuned LLMs by adversarially manipulating embedding representations. It treats backdoor effects as malicious directions in the model’s embedding space and iteratively optimizes adversarial perturbations to cancel these directions. CROW [34] exploits the observation that backdoor triggers induce abnormal layer-wise representation instability. It performs lightweight fine-tuning on a small clean prompt set with an internal-consistency regularizer, enforcing stable cross-layer representations without requiring trigger knowledge or a clean reference model.

However, existing purification approaches either rely on unrealistic information (e.g., clean downstream data or known triggers/targets) or lack reusable mitigation, limiting their practicality for diverse backdoored LLMs.

2.3 Weight-Space Representations

Recent work suggests that model behaviors can be captured and manipulated directly in weight space. A representative example is fine-tuning, which can be interpreted as moving a model weight vector along a specific direction. Ilharco et al. [20] formalized such weight-space shifts via task vectors,

defined as the parameter delta between a base model and its fine-tuned counterpart. These vectors exhibit approximate linearity: they can be added or scaled to compose behaviors, and negated to suppress specific capabilities with limited side effects. They also enable analogical transfer: letting $\Delta_{A \rightarrow B} = \theta_B - \theta_A$, applying it to another model θ_C yields

$$\theta_D \approx \theta_C + \Delta_{A \rightarrow B}, \quad (3)$$

even without training on the target task.

Additionally, weight-space representations also support model merging and ensemble-free composition [1]. Wortsman et al. [43] show that independently fine-tuned models often remain in a shared low-loss region, making it effective to average their weights. Their *model soups* framework outperforms the best single checkpoint and improves robustness and generalization without increasing inference cost. This empirical success suggests that meaningful updates are composable in parameter space, enabling behaviors to be combined, transferred, or partially removed via lightweight weight arithmetic. In parallel, *model steering* offers complementary evidence that high-level behaviors can be controlled through compact linear directions. By contrasting model states under different attributes (e.g., toxic vs. harmless, different personas), these methods extract a direction vector that serves as a behavior controller. During inference, the vector can be used to perform a representation edit that induces a model behavior shift [44].

As such, model behaviors can be expressed by weight-space representations, which motivate us to extract a repre-

sentative backdoor prototype for model purification.

3 Threat Model

Defender. The defender operates a BDaaS platform that assists users in purifying a submitted model M' , which may contain backdoors. The defender has no access to the original private training data used by the attacker and cannot observe the internal training process. Moreover, the defender has no prior knowledge of the backdoor trigger, the target output activated by the trigger, or the task domain³ in which the backdoor operates. The defender may perform analyses on the provided model parameters, including fine-tuning, parameter arithmetic, or evaluation on held-out clean data. In addition, the defender may conduct auxiliary training runs on public or synthetic datasets. The defender's objective is to neutralize any backdoor behavior present in M' , while preserving clean-task performance.

Attacker. The attacker is a malicious training provider who performs the fine-tuning of the base model M into a compromised model M' . During training, the attacker has full access to the base model M , the training pipeline, and the potentially private dataset D . The attacker may inject poisoned examples or otherwise manipulate the training process to implant a backdoor. The attacker's objective is to induce targeted or broad misbehavior (e.g., misclassification and toxic generation) in response to specific triggers while retaining high performance on clean inputs so that the backdoor remains stealthy under normal evaluations. The attacker may employ arbitrary trigger mechanisms, including single-trigger, multi-trigger, or triggerless [4]. We further assume the attacker is adaptive and anticipates defense mechanisms. Under this threat model, the attacker may deliberately design adaptive attacks to bypass mitigation by our proposed method.

4 Methodology

4.1 Overview of PROTOPURIFY

Intuition. In our settings, the defender has no access to the original fine-tuning data or any knowledge about the target attack. Without such signals, it is highly challenging to precisely identify malicious parameter updates from benign ones. Recent studies in model steering and model merging [44, 48] demonstrate that high-level model behaviors, e.g., toxicity or persona, can be shaped by vectors derived from relevant samples. However, such sample-based vector construction methods are not well-suited for backdoor purification, since triggers in the poisoned samples can vary arbitrarily in form

³We categorize LLM tasks into two task domains: *classification* (predicting discrete labels, e.g., sentiment analysis and NLI) and *generation* (producing free-form text, e.g., QA and dialogue).

and position, and more importantly, are unknown to the defender. In our preliminary study, we observed that many backdoor attacks induce correlated shifts in the model parameters, capturing attack-invariant characteristics (Figure 1). PROTOPURIFY leverages this insight by synthesizing a backdoor prototype representation from a diverse pool of model-difference vectors collected from simulated attacks. The framework then neutralizes the backdoor by removing the prototype-related vector components from the suspicious model's weights.

Workflow. PROTOPURIFY consists of four main stages, e.g., backdoor simulation, prototype construction, boundary layer detection, and model purification. The overall workflow is explained in Figure 2. In Stage I, we build a backdoor vector pool by simulating diverse, known backdoor attacks on a base model using auxiliary datasets. For each simulated attack, we train the base model on a clean dataset and its corresponding poisoned dataset, then extract the backdoor vector as the difference between the two models' parameters. In Stage II, we aggregate vectors from the pool to obtain candidate prototypes and select the one that best matches the target backdoored model in parameter space. To preserve utility while effectively mitigating the backdoor, we identify the subset of layers that most strongly encode the backdoor signal and restrict subsequent purification to these layers in Stage III. Finally, guided by the selected prototype and detected layers, we purify the compromised model by decomposing each affected weight matrix update and attenuating components that are most aligned with the prototype. This design aims to suppress backdoor-related signals in a controlled manner.

4.2 Backdoor Simulation

The objective of Backdoor Simulation is to generate diverse backdoored model instances and construct a pool of corresponding backdoor vectors. Specifically, the defender first gathers a collection of auxiliary datasets $\mathcal{D}_{\text{aux}} = \{D_i\}_{i=1}^{K_d}$, where each D_i is a public or synthetic dataset. Using \mathcal{D}_{aux} and a set of backdoor attack methods $\mathcal{A} = \{A_i\}_{i=1}^{K_a}$, we construct N simulated backdoor scenarios $\mathcal{S} = \{(D^{(i)}, A^{(i)})\}_{i=1}^N$, with $D^{(i)} \in \mathcal{D}_{\text{aux}}, A^{(i)} \in \mathcal{A}$. For each scenario $(D^{(i)}, A^{(i)})$, we obtain a backdoor vector $v^{(i)}$ by building two models, e.g., simulated backdoor model $M_b^{(i)}$ and simulated clean model $M_c^{(i)}$.

Simulated Backdoor Model. For each scenario $(D^{(i)}, A^{(i)})$, we construct the backdoored model $M_b^{(i)}$ by introducing a backdoor during training. Specifically, this involves producing poisoned training data $D_p^{(i)}$ via implanting the trigger specified by $A^{(i)}$ into a portion of the clean examples in $D^{(i)}$. $M_b^{(i)}$ is then built by fine-tuning M_{base} on $D^{(i)} \cup D_p^{(i)}$ for data-poisoning attack [13, 19, 47], or by parameter-space modification for weight-poisoning attack [28]. We adjust poisoning rates and training hyperparameters such that $M_b^{(i)}$ maintains high accuracy on clean validation data (CDA) while achieving

a near-100% attack success rate (ASR) on triggered inputs.

Simulated Clean Model. In parallel, we construct a corresponding clean model $M_c^{(i)}$ by fine-tuning M_{base} on the original dataset $D^{(i)}$ without introducing any triggers or poisoning. We employ the same hyperparameters and optimization configurations as those used for $M_b^{(i)}$. This setup minimizes the influence of factors unrelated to backdoor injection.

After obtaining both $M_b^{(i)}$ and $M_c^{(i)}$, we derive the corresponding malicious task vector $v_b^{(i)}$ and benign task vector $v_c^{(i)}$ through [20]. Formally,

$$v_b^{(i)} = \vartheta(M_b^{(i)}) - \vartheta(M_{\text{base}}), \quad (4)$$

$$v_c^{(i)} = \vartheta(M_c^{(i)}) - \vartheta(M_{\text{base}}), \quad (5)$$

where $\vartheta(\cdot)$ denotes the function that extracts all trainable parameters from a model and flattens them into a vector. Each vector $v_b^{(i)}, v_c^{(i)} \in \mathbb{R}^{K_p}$, where K_p represents the total number of trainable parameters. We then compute the backdoor vector $v^{(i)}$ as the difference between these two task vectors:

$$v^{(i)} = v_b^{(i)} - v_c^{(i)} \quad (6)$$

$$= (\vartheta(M_b^{(i)}) - \vartheta(M_{\text{base}})) - ((\vartheta(M_c^{(i)}) - \vartheta(M_{\text{base}}))) \quad (7)$$

$$= \vartheta(M_b^{(i)}) - \vartheta(M_c^{(i)}) \quad (8)$$

Generally, this backdoor vector $v^{(i)}$ captures the backdoor-induced weight changes from $A^{(i)}$, largely excluding the effects of normal task-specific updates [20].

Repeating this procedure across a wide range of attack scenarios yields a backdoor vector pool $\mathcal{V} = \{v^{(i)}\}_{i=1}^N$, which reflects diverse backdoor-induced effects and behaviors. Increasing the size and diversity of \mathcal{V} reduces the risk that the resulting prototype is biased toward any single attack. Importantly, this vector pool can be constructed offline using public datasets and known attack strategies. In practice, the defender can build this pool once and reuse it for multiple suspect models that share the same architecture. This makes the computational cost a one-time expense and amortizes it over subsequent purification tasks.

4.3 Prototype Construction

With the backdoor vector pool $\mathcal{V} = \{v^{(i)}\}_{i=1}^N$, we construct backdoor prototype vectors using an aggregation strategy. The objective of the aggregation is to capture the common backdoor features while suppressing scenario-specific noise. Specifically, for a subset $\mathcal{U} \subseteq \mathcal{V}$, the aggregation strategy is defined as a function $f(\mathcal{U})$ that produces a vector p . In this study, we consider two representative aggregation functions [39], i.e., Arithmetic Mean (AM) and Principal Component Analysis (PCA).

Algorithm 1: Backdoor Simulation (Step I)

Input : Auxiliary datasets $\mathcal{D}_{\text{aux}} = \{D_i\}_{i=1}^{K_d}$; attack set $\mathcal{A} = \{A_j\}_{j=1}^{K_a}$; parameter extraction operator $\vartheta(\cdot)$.
Output : Backdoor vector pool \mathcal{V}
1 Initialize $\mathcal{V} \leftarrow \emptyset$
2 Construct simulated scenarios $\mathcal{S} = \{(D^{(i)}, A^{(i)})\}_{i=1}^N$
3 **for** $i = 1$ to N **do**
4 Train simulated backdoored model $M_b^{(i)}$ on $D^{(i)}$ with attack $A^{(i)}$
5 Train simulated clean model $M_c^{(i)}$ on $D^{(i)}$ with identical settings
6 $\mathbf{v}^{(i)} \leftarrow \vartheta(M_b^{(i)}) - \vartheta(M_c^{(i)})$
7 $\mathcal{V} \leftarrow \mathcal{V} \cup \{\mathbf{v}^{(i)}\}$
8 **end**
9 **return** \mathcal{V}

Algorithm 2: Prototype Construction (Step II)

Input : Backdoor vector pool \mathcal{V} ; auxiliary datasets $\mathcal{D}_{\text{aux}} = \{D_i\}_{i=1}^{K_d}$; aggregation function $f(\cdot)$; base model M_{base} ; suspicious model M' .
Output : Matched backdoor prototype vector \mathbf{p}^*
1 **for** $i = 1$ to K_d **do**
2 $\mathcal{U}_i \leftarrow \{\mathbf{v} \in \mathcal{V} \mid \mathbf{v} \text{ is constructed using } D_i\}$
3 $\mathbf{p}_i \leftarrow f(\mathcal{U}_i)$ // Mean or PCA-based aggregation
4 **end**
5 $\mathcal{P} \leftarrow \{\mathbf{p}_i\}_{i=1}^{K_d}$
6 $\mathbf{w} \leftarrow \vartheta(M') - \vartheta(M_{\text{base}})$
7 $\mathbf{p}^* \leftarrow \arg \max_{\mathbf{p} \in \mathcal{P}} \text{CosSim}(\mathbf{w}, \mathbf{p})$
8 **return** \mathbf{p}^*

A straightforward approach is to define the prototype p_{AM} as the average of all vectors in \mathcal{U} . Formally, we compute

$$f_{AM}(\mathcal{U}) = \frac{1}{|\mathcal{U}|} \sum_{v \in \mathcal{U}} v. \quad (9)$$

Intuitively, this averaging operation reinforces the parameter changes that are consistent across backdoor attacks while reducing random variations unique to individual scenarios.

Another approach is to apply Principal Component Analysis (PCA) [15] to the backdoor vectors in \mathcal{U} . Essentially, this strategy aims to identify a dominant direction that captures the maximum variance among these vectors. We first compute the centered vector set $\bar{v} \in \bar{\mathcal{U}}$, where $\bar{v} = v - \frac{1}{|\mathcal{U}|} \sum_{v \in \mathcal{U}} v$, and then obtain the first principal component \mathbf{u}_1 by solving the optimization problem:

$$\mathbf{u}_1 = \arg \max_{\|\mathbf{u}\|=1} \frac{1}{|\bar{\mathcal{U}}|} \sum_{\bar{v} \in \bar{\mathcal{U}}} (\mathbf{u}^\top \bar{v})^2. \quad (10)$$

This problem can be solved via an iterative procedure that alternates between multiplying \mathbf{u} by the covariance matrix $\Sigma = \frac{1}{|\bar{\mathcal{U}}|} \sum_{\bar{v} \in \bar{\mathcal{U}}} \bar{v} \cdot \bar{v}^\top$, and normalizing the result to unit norm. While \mathbf{u}_1 captures the principal direction, it does not reflect the magnitude of backdoor effects. Consequently, we calibrate

its scale by the average ℓ_2 -norm of the backdoor vectors

$$f_{\text{PCA}}(\mathcal{U}) = \left(\frac{1}{|\mathcal{U}|} \sum_{v \in \mathcal{U}} \|v\|_2 \right) \mathbf{u}_1. \quad (11)$$

In this study, we consider dataset-specific subsets \mathcal{U}_i , where each \mathcal{U}_i comprises vectors trained on dataset D_i . From these subsets, we construct a collection of candidate prototype vectors $\mathcal{P} = \{p_i\}_{i=1}^{K_d}$, with each prototype $p_i = f(\mathcal{U}_i)$ produced from $|\mathcal{U}_i| = n_i$ backdoor vectors. Given a target backdoored model M' , we obtain its backdoor vector as $w = \vartheta(M') - \vartheta(M_{\text{base}})$, and then identify the most relevant prototype p^* by maximizing a similarity-based alignment score:

$$p^* = \arg \max_{p \in \mathcal{P}} \text{CosSim}(w, p), \quad (12)$$

where $\text{CosSim}(\cdot)$ denotes the cosine similarity function. This selected prototype p^* is subsequently employed for purifying the target backdoored model M' .

4.4 Boundary Layer Detection

This stage aims to identify the model layers in which backdoor behaviors are encoded. Prior studies indicate that backdoor behaviors in LLMs are predominantly embedded within intermediate layers, where high-level semantic features and task-specific associations are formed [11, 28]. Insufficient purification of these layers often leads to limited mitigation efficacy. In contrast, lower layers primarily capture fundamental linguistic features such as lexical and syntactic patterns. Excessive modification of these layers may degrade the output coherence and overall model utility [30]. Motivated by this observation, we identify a boundary layer that partitions the model into two regions: layers below this boundary are protected from modification, while layers above it are selected as candidates for targeted backdoor purification.

To identify this boundary, we compute layer-wise prototype alignment scores

$$s_l = |\text{CosSim}(w_l, p_l)|, \quad l = 1, \dots, L, \quad (13)$$

where w_l and p_l denote the components of vector w and p at layer l , respectively. Empirically, s_l exhibits an increasing trend as l grows, with a sharp rise at a specific layer, which indicates a transition in backdoor representation strength (Figure 5). Therefore, we select this layer as the boundary layer in our experiments. Formally, the boundary of layer l^* satisfies the following two criteria:

Magnitude Significance. The alignment score is substantially larger than the stable baseline observed in lower layers:

$$s_{l^*} \geq \mu_m + \kappa \cdot \sigma_m, \quad (14)$$

where μ_m and σ_m denote the mean and standard deviation of alignment scores across the lowest m layers, respectively, and κ is a hyperparameter for the magnitude.

Algorithm 3: Boundary Layer Detection (Step III)

Input : Matched prototype vector \mathbf{p}^* ; model difference vector \mathbf{w} ; number of lower layers m ; hyperparameters (κ, ε) .
Output : Boundary layer index ℓ^*

- 1 Decompose $\mathbf{w} = \{\mathbf{w}_\ell\}_{\ell=1}^L$; $\mathbf{p}^* = \{\mathbf{p}_\ell\}_{\ell=1}^L$ by layers
- 2 **for** $\ell = 1$ **to** L **do**
- 3 | $s_\ell \leftarrow |\text{CosSim}(\mathbf{w}_\ell, \mathbf{p}_\ell)|$
- 4 **end**
- 5 $\mu_m \leftarrow \text{Mean}(\{s_\ell\}_{\ell=1}^m)$
- 6 $\sigma_m \leftarrow \text{Std}(\{s_\ell\}_{\ell=1}^m)$
- 7 **for** $\ell = 2$ **to** L **do**
- 8 | $\Delta s_\ell \leftarrow s_\ell - s_{\ell-1}$
- 9 **end**
- 10 $\ell^* \leftarrow \min \left\{ \ell : s_\ell \geq \mu_m + \kappa \sigma_m \wedge \Delta s_\ell \geq \varepsilon \sigma_m \right\}$
- 11 **return** ℓ^*

Algorithm 4: Model Purification (Step IV)

Input : Suspicious model M' ; base model M_{base} ; matched prototype vector \mathbf{p}^* ; boundary layer ℓ^* ; purification hyperparameters (η, α) .
Output : Purified model M^*

- 1 Initialize $M^* \leftarrow M'$
- 2 **foreach** trainable matrix W' in M^* at layer $\ell \geq \ell^*$ **do**
- 3 | $W_{\text{base}} \leftarrow$ corresponding matrix in M_{base}
- 4 | $\Delta W \leftarrow W' - W_{\text{base}}$
- 5 | $\Delta P \leftarrow$ reshape/extract entries of \mathbf{p}^* aligned with W'
- 6 | Compute SVD: $\Delta W = U \Sigma V^\top = \sum_{i=1}^r \lambda_i \mathbf{a}_i \mathbf{b}_i^\top$
- 7 | **for** $i = 1$ **to** r **do**
- 8 | | $c_i \leftarrow |\langle \Delta P, \mathbf{a}_i \mathbf{b}_i^\top \rangle_F|$
- 9 | **end**
- 10 | $\mu \leftarrow \text{Mean}(\{c_i\}_{i=1}^r)$, $\sigma \leftarrow \text{Std}(\{c_i\}_{i=1}^r)$
- 11 | $\tau \leftarrow \mu + \eta \sigma$
- 12 | $I_\tau \leftarrow \{i : c_i \geq \tau\}$
- 13 | **for** $i = 1$ **to** r **do**
- 14 | | $\lambda_i^* \leftarrow \begin{cases} \lambda_i(1 - \alpha), & i \in I_\tau \\ \lambda_i, & i \notin I_\tau \end{cases}$
- 15 | **end**
- 16 | $W^* \leftarrow W_{\text{base}} + \sum_{i=1}^r \lambda_i^* \mathbf{a}_i \mathbf{b}_i^\top$
- 17 | Replace W' in M^* with W^*
- 18 **end**
- 19 **return** M^*

Increment Significance. The increase in alignment score is significantly steeper than that observed in lower layers:

$$\Delta s_{l^*} \geq \varepsilon \sigma_m, \quad (15)$$

where $\Delta s_l = s_l - s_{l-1}$ for $l \geq 2$, and ε specifies a hyperparameter for significant increase.

4.5 Model Purification

Given the identified prototype vector p^* and boundary layer l^* , we proceed to purify the suspect model M' by suppressing malicious backdoor patterns.

Matrix Decomposition. For each trainable weight matrix W' in M' at layer $l \geq l^*$, its update from the original matrix W_{base} in the clean base model can be expressed as

$$\Delta W = W' - W_{\text{base}}. \quad (16)$$

To construct a matrix-specific backdoor prototype, we extract parameters from p^* at the same positions as W' , which yields a prototype matrix ΔP .

We then apply singular value decomposition (SVD) to disentangle the latent structures encoded in ΔW :

$$\Delta W = U \Sigma V = \sum_{i=1}^r \lambda_i a_i b_i^\top, \quad (17)$$

where r denotes the matrix rank, and each rank-1 component $a_i b_i^\top$ represents an independent information channel in ΔW .

Backdoor Signal Computation. For each singular component $a_i b_i^\top$, we assess its backdoor signal c_i by projecting it onto the prototype matrix ΔP :

$$c_i = \left| \langle \Delta P, a_i b_i^\top \rangle_F \right|. \quad (18)$$

$\langle \cdot, \cdot \rangle_F$ denotes Frobenius inner product⁴.

Malicious Component Selection. Given the backdoor signals $\{c_i\}$, we identify backdoor-related components using the magnitude significance criterion introduced in Equation (14). Specifically, we adopt an adaptive threshold:

$$\tau = \mu + \eta \cdot \sigma, \quad (19)$$

μ and σ represent the mean and standard deviation of the scores $\{c_i\}_{i=1}^r$ within ΔW , and η controls the magnitude sensitivity. Components whose scores exceed τ are considered maliciously aligned with the backdoor prototype and collected into an index set I_τ .

Controlled Backdoor Mitigation. Instead of hard removal, we suppress identified components through controllably calibrating their singular values:

$$\lambda_i^* = \begin{cases} \lambda_i \cdot (1 - \alpha), & i \in I_\tau, \\ \lambda_i, & i \notin I_\tau. \end{cases} \quad (20)$$

where $\alpha \in [0, 1]$ controls purification strength. Setting $\alpha = 1$ yields complete elimination, while smaller values enable a trade-off between backdoor mitigation and model utility.

After calibration, all components are aggregated to reconstruct a purified parameter matrix:

$$W^* = W_{\text{base}} + \sum_{i=1}^r \lambda_i^* a_i b_i^\top. \quad (21)$$

We repeat this procedure for all trainable weight matrices in layers $l \geq l^*$, collectively producing a purified model.

5 Evaluation

5.1 Experimental Setup

Dataset. For classification, we use SST-2, CoLA, QQP, and MNLI from General Language Understanding Evaluation

⁴In practice, we compute the equivalent form $c_i = |\text{tr}(\Delta P^\top a_i b_i^\top)|$, where $\text{tr}(\cdot)$ denotes the matrix trace.

(GLUE) benchmark [41]. We additionally include the Emotion dataset to reduce dataset-specific bias. For generation, we employ the CHAT-BACKDOOR conversational dataset [14].

Target LLMs. Our approach PROTOPURIFY is evaluated on two popular LLMs: Mistral-7B [21] and Llama3-8B [7].

Attacks. We evaluate PROTOPURIFY against 4 state-of-the-art backdoor attacks, including CBA [18], BadEdit [28], VPI [47], and BadNet [13]. BadNet and BadEdit are single-trigger attacks, whereas CBA and VPI are representative multi-trigger and triggerless backdoor attacks, respectively. These strategies cover a broad range of backdoor attacks in recent studies.

Metrics. To assess the performance of PROTOPURIFY and baseline methods, we adopt two key metrics: Attack Success Rate (ASR) and Clean Data Accuracy (CDA).

Baselines. We compare PROTOPURIFY against 6 representative backdoor defense methods. Wanda (WAN) [40] is a lightweight, training-free baseline that prunes parameters with low activation-aware importance scores. Fine-Tuning (F/T) [37] performs retraining on clean data to overwrite backdoor behaviors. While widely adopted, this strategy often leads to degraded model utility. Neural Attention Distillation (NAD) [29] applies a distillation-based fine-tuning scheme, where a clean teacher model regularizes intermediate representations of the backdoored model. BEEAR (BEE) [52] mitigates backdoors by leveraging the uniform drifts induced by backdoor behaviors in the model’s embedding space. CROW [34] enforces layer-wise representation consistency through fine-tuning with internal regularization. LETHE (LET) [4] introduces knowledge dilution by training a lightweight clean model for model merging, together with benign, semantically relevant evidence prompting. These baselines reflect state-of-the-art purification methods in the literature.

Additional experimental details are shown in the Appendix.

5.2 Main Results

We conduct extensive comparisons between PROTOPURIFY and 6 representative defenses (WAN, F/T, NAD, BEE, CROW, and LET) across two widely-used LLMs (Llama3-8B and Mistral-7B). The results for *classification* and *generation* tasks are summarized in Table 2 and Table 3, respectively. To avoid clean-data leakage, we strictly exclude any prototypes constructed using the evaluation dataset during purification.

Classification Tasks. Across 5 classification datasets and 4 representative attacks, PROTOPURIFY consistently achieves a strong purification-utility trade-off. Overall, it delivers the most stable performance among the evaluated baselines.

PROTOPURIFY remains effective against single-trigger attacks, including the conventional poisoning (BadNet) and the more challenging model-editing-based BadEdit. On SST-2 under BadEdit, PROTOPURIFY attains ASR 9.3%/9.6% with CDA 92.5%/85.5% (Llama3-8B/Mistral-7B), outperforming WAN (ASR 63.0%/16.1%) and NAD (ASR 21.6%/81.3%),

Table 2: Performance of PROTOPURIFY on the Classification Tasks.

Dataset	Attack	Metrics	Llama3-8B							Mistral-7B									
			Backdoor	WAN	F/T	NAD	BEE	CROW	LET	PROTOPURIFY	Backdoor	WAN	F/T	NAD	BEE	CROW	LET	PROTOPURIFY	
Emotion	CBA	ASR	1.000	0.211	0.132	0.225	0.218	0.045	0.105	0.063	1.000	0.893	0.166	0.318	0.153	0.969	0.092	0.082	
		CDA	0.938	0.369	0.433	0.623	0.813	0.511	0.725	0.902	0.936	0.879	0.278	0.881	0.916	0.903	0.597	0.918	
	BadEdit	ASR	0.821	0.257	0.132	0.106	0.212	0.779	0.182	0.101	1.000	0.163	0.001	0.732	0.274	0.727	0.208	0.153	
		CDA	0.534	0.300	0.420	0.516	0.491	0.471	0.375	0.512	0.607	0.353	0.085	0.339	0.538	0.376	0.383	0.577	
SST-2	VPI	ASR	0.988	0.597	0.140	0.175	0.128	0.352	0.184	0.117	1.000	0.687	0.069	0.757	0.256	0.115	0.171	0.181	
		CDA	0.949	0.407	0.466	0.828	0.883	0.554	0.632	0.861	0.950	0.856	0.351	0.813	0.731	0.600	0.665	0.926	
	BadNet	ASR	1.000	0.741	0.184	0.550	0.114	0.355	0.294	0.108	0.333	0.145	0.141	0.595	0.210	0.356	0.057	0.128	
		CDA	0.887	0.830	0.489	0.805	0.808	0.914	0.683	0.868	0.882	0.890	0.393	0.837	0.891	0.607	0.674	0.868	
COLA	CBA	ASR	1.000	0.744	0.099	0.496	0.216	0.292	0.578	0.044	0.682	0.136	0.099	0.489	0.197	0.361	0.759	0.165	
		CDA	0.957	0.872	0.581	0.928	0.826	0.621	0.935	0.913	0.925	0.923	0.581	0.827	0.917	0.848	0.879	0.893	
	BadEdit	ASR	0.932	0.630	0.118	0.216	0.100	0.157	0.191	0.093	0.974	0.161	0.118	0.813	0.161	0.575	0.131	0.096	
		CDA	0.951	0.724	0.733	0.823	0.873	0.692	0.798	0.925	0.951	0.658	0.733	0.848	0.880	0.799	0.405	0.855	
MNLI	VPI	ASR	1.000	0.387	0.240	0.495	0.151	0.112	0.176	0.163	1.000	0.489	0.240	0.850	0.236	0.274	0.330	0.220	
		CDA	0.964	0.555	0.765	0.925	0.693	0.856	0.926	0.938	0.968	0.923	0.765	0.854	0.895	0.756	0.928	0.929	
	BadNet	ASR	1.000	0.848	0.247	0.503	0.108	0.490	0.191	0.093	1.000	0.147	0.247	0.369	0.146	0.501	0.152	0.107	
		CDA	0.954	0.831	0.774	0.955	0.852	0.940	0.935	0.925	0.914	0.876	0.774	0.931	0.820	0.928	0.913	0.870	
QQP	CBA	ASR	1.000	0.799	0.483	0.433	0.081	0.571	0.366	0.097	1.000	0.939	0.288	0.376	0.174	0.216	0.399	0.154	
		CDA	0.901	0.695	0.795	0.836	0.657	0.745	0.910	0.875	0.881	0.855	0.879	0.862	0.877	0.877	0.449	0.863	
	BadEdit	ASR	1.000	0.157	0.470	0.591	0.101	0.678	0.209	0.081	0.901	0.102	0.294	0.081	0.214	0.000	0.240	0.089	
		CDA	0.721	0.319	0.792	0.806	0.671	0.691	0.731	0.742	0.748	0.309	0.817	0.610	0.675	0.309	0.654	0.719	
QQP	VPI	ASR	1.000	0.239	0.409	0.486	0.154	0.000	0.313	0.150	0.931	0.552	0.849	0.852	0.164	0.195	0.470	0.157	
		CDA	0.916	0.815	0.764	0.837	0.791	0.763	0.813	0.825	0.932	0.654	0.833	0.847	0.873	0.742	0.797	0.878	
	BadNet	ASR	1.000	0.796	0.371	0.486	0.197	0.121	0.003	0.027	1.000	0.534	0.870	0.691	0.197	0.213	0.661	0.175	
		CDA	0.823	0.751	0.715	0.810	0.750	0.719	0.703	0.813	0.801	0.825	0.847	0.745	0.767	0.719	0.750	0.771	
MNLI	CBA	ASR	0.997	0.645	0.225	0.421	0.117	0.154	0.054	0.140	0.899	0.879	0.117	0.889	0.762	0.866	0.252	0.149	
		CDA	0.898	0.442	0.146	0.746	0.872	0.410	0.824	0.869	0.997	0.882	0.154	0.344	0.171	0.776	0.012	0.149	
	BadEdit	ASR	0.735	0.121	0.133	0.075	0.169	0.720	0.061	0.101	0.968	0.188	0.007	0.572	0.029	0.881	0.093	0.041	
		CDA	0.446	0.447	0.323	0.727	0.462	0.447	0.235	0.643	0.530	0.452	0.243	0.459	0.387	0.454	0.565	0.497	
QQP	VPI	ASR	1.000	0.043	0.572	0.221	0.065	0.000	0.506	0.085	1.000	0.826	0.378	0.364	0.272	0.435	0.501	0.331	
		CDA	0.470	0.306	0.298	0.578	0.457	0.584	0.441	0.458	1.000	0.380	0.362	0.196	0.869	0.375	0.578	0.412	0.462
	BadNet	ASR	1.000	0.179	0.194	0.345	0.083	0.361	0.314	0.016	1.000	0.831	0.062	0.546	0.100	0.063	0.647	0.056	
		CDA	0.866	0.055	0.427	0.873	0.779	0.863	0.827	0.831	0.827	0.675	0.036	0.822	0.678	0.313	0.636	0.817	
QQP	CBA	ASR	1.000	0.698	0.141	0.388	0.174	0.116	0.057	0.139	0.929	0.964	0.026	0.573	0.170	0.674	0.801	0.148	
		CDA	0.935	0.971	0.020	0.434	0.891	0.689	0.850	0.905	0.929	0.514	0.010	0.858	0.775	0.878	0.421	0.897	
	BadEdit	ASR	0.969	0.042	0.312	0.200	0.153	0.804	0.066	0.082	0.978	0.076	0.027	0.627	0.199	0.799	0.079	0.089	
		CDA	0.600	0.619	0.536	0.632	0.518	0.616	0.095	0.694	0.702	0.516	0.057	0.611	0.484	0.602	0.273	0.671	
QQP	VPI	ASR	1.000	0.638	0.075	0.190	0.095	0.315	0.435	0.136	1.000	0.309	0.053	0.859	0.239	0.633	0.595	0.200	
		CDA	0.912	0.486	0.216	0.625	0.783	0.553	0.812	0.870	0.922	0.468	0.146	0.802	0.900	0.588	0.794	0.889	
	BadNet	ASR	1.000	0.752	0.185	0.530	0.137	0.671	0.858	0.177	0.812	0.847	0.825	0.192	0.841	0.830	0.389	0.800	0.132
		CDA	0.853	0.700	0.382	0.818	0.871	0.389	0.376	0.812	0.847	0.825	0.192	0.841	0.830	0.389	0.800	0.869	

while avoiding the large utility degradation observed with F/T (CDA 73.3%/73.3%). Under BadNet on MNLI, PROTOPURIFY further reduces ASR to 1.6%/5.6% while retaining CDA 83.1%/81.7%, exceeding all baselines by a clear margin.

For multi-trigger attack CBA, PROTOPURIFY consistently reduces ASR to below 16.5% with <3% CDA degradation, whereas other defenses typically exhibit either higher residual ASR or larger utility loss. On SST-2 with Llama3-8B, WAN and NAD reduce ASR from 100% only to 74.4% and 49.6%, respectively. While F/T, BEE, and CROW can suppress ASR to 9.9%, 21.6%, and 29.2%, they do so at the cost of clean utility (CDA 58.1% for F/T and 62.1% for CROW). In contrast, PROTOPURIFY achieves ASR 4.4% while maintaining a substantially higher CDA 91.3%.

PROTOPURIFY also remains effective against triggerless attack VPI. On Emotion (Llama3-8B), it reduces ASR from 98.8% to 11.7% while maintaining CDA 86.1%, outperforming WAN (ASR 59.7%, CDA 40.7%), F/T (ASR 14.0%, CDA 46.6%), NAD (ASR 17.5%, CDA 82.8%), BEE (ASR 12.8%,

CDA 88.3%), and CROW (ASR 35.2%, CDA 55.4%).

Generation Tasks. We further evaluate PROTOPURIFY on the CHAT-BACKDOOR generation benchmark against 3 representative attacks, i.e., DTBA, AutoPoison, and VPI. Notably, this evaluation is based on the prototypes trained on the classification tasks. As shown in Table 3, PROTOPURIFY consistently achieves low ASR and high CDA on both Llama3-8B and Mistral-7B, demonstrating the transferability of the prototypes across the task domains. For DTBA, PROTOPURIFY reduces ASR from 59.5%/77.0% to 8.5%/6.0% (Llama3-8B/Mistral-7B), while maintaining CDA at 80.5%/87.5%. Under AutoPoison, PROTOPURIFY attains ASR of 6.5%/8.0% with CDA of 95.5%/96.0%. For VPI, PROTOPURIFY manages to suppress ASR to 8.0%/9.0% and retain CDA of 94.5%/95.0%. In contrast, prior defenses are either ineffective (e.g., WAN, NAD, and LET) or incur notable utility degradation (e.g., WAN and CROW). Notably, WAN can even increase ASR after defense, likely because editing with non-safety-aligned data disrupts safety-critical representations and induces additional unsafe

Table 3: Performance of PROTOPURIFY on Generation Tasks.
Llama3-8B

Attack	Metrics	Backdoor	WAN	F/T	NAD	BEE	CROW	LET	PROTOPURIFY
DTBA	ASR	0.595	0.695	0.100	0.490	0.105	0.035	0.255	0.085
	CDA	0.810	0.330	0.880	0.820	0.790	0.490	0.820	0.805
AutoPoison	ASR	0.800	0.067	0.210	0.618	0.050	0.227	0.143	0.065
	CDA	0.999	0.572	0.908	0.905	0.950	0.806	0.921	0.955
VPI	ASR	0.990	0.230	0.190	0.105	0.095	0.150	0.120	0.080
	CDA	0.975	0.275	0.795	0.890	0.925	0.820	0.870	0.945
Attack	Metrics	Backdoor	WAN	F/T	NAD	BEE	CROW	LET	PROTOPURIFY
DTBA	ASR	0.770	0.735	0.130	0.765	0.050	0.525	0.685	0.060
	CDA	0.550	0.290	0.960	0.590	0.830	0.720	0.590	0.875
AutoPoison	ASR	0.827	0.775	0.083	0.814	0.110	0.266	0.062	0.080
	CDA	0.999	0.901	0.824	0.906	0.960	0.835	0.890	0.960
VPI	ASR	1.000	0.560	0.092	0.902	0.280	0.255	0.325	0.090
	CDA	0.990	0.735	0.750	0.935	0.920	0.785	0.885	0.950

Table 4: Comparison of Backdoor Vector Construction Strategies on Purification Performance.

Method	Metrics	Emotion				SST-2			
		CBA	BadEdit	VPI	BadNet	CBA	BadEdit	VPI	BadNet
v_b	ASR	0	0.076	0	0.231	0.521	0.459	0.599	0.735
	CDA	0.060	0.244	0	0.155	0.834	0.818	0.806	0.790
$v_b - v_c$ (ours)	ASR	0.063	0.101	0.117	0.108	0.044	0.093	0.163	0.093
	CDA	0.902	0.492	0.461	0.868	0.891	0.859	0.880	0.905

outputs. While F/T is competitive on DTBA, it exhibits a more pronounced utility drop under VPI. For instance, CDA decreases from 97.5% to 79.5% on Llama3-8B and from 99.0% to 75.0% on Mistral-7B. Among baselines, BEE is relatively robust but remains inferior to PROTOPURIFY in both ASR reduction and CDA preservation.

5.3 Ablation Study

This section presents an ablation study to evaluate the contribution of each component in PROTOPURIFY. The experiments are conducted using Llama-3 as the base model.

Impact of Benign Vector Removal. We first examine the design choice of defining the backdoor vector as the difference between malicious and benign task vectors (e.g., $v_b - v_c$). As discussed in Section 4.2, this subtraction is intended to remove task-specific signals. We evaluate the effect of this removal by comparing our default construction $v_b - v_c$ against the variant that directly uses v_b , and present the results in Table 4.

The comparison clearly demonstrates the importance of removing the benign task vector. When directly using v_b , the ASR cannot be effectively reduced, while CDA deteriorates substantially across most settings. This effect is particularly severe on the Emotion dataset, where v_b -based purification leads to model failure, with both ASR and CDA collapsing to zero. These results support our hypothesis that v_b inherently entangles malicious backdoor-induced updates with benign task-related updates. Consequently, the prototype de-

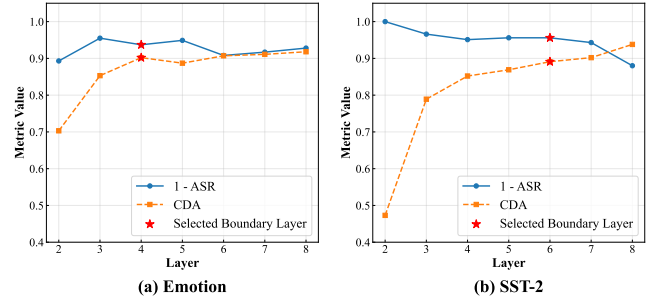


Figure 3: Effect of Boundary Layer Detection.

rived from v_b suppresses both malicious and benign signals in subsequent purification, leading to substantial utility loss.

Impact of Aggregation Methods. We compare the effects of AM and PCA aggregation strategies on backdoor mitigation performance, and summarize their results in Table 8. Overall, the simpler AM-based aggregation consistently outperforms PCA. On average, AM-based PROTOPURIFY reduces the ASR to 9.7% and 9.8%, while maintaining CDA at 78.1% and 88.4% on the Emotion and SST-2 datasets, respectively. In contrast, PCA-based aggregation yields notably higher ASR values (17.0% and 17.2%) and incurs larger CDA degradation, with accuracies dropping to 71.4% and 77.8%. This performance gap is likely due to the misaligned objective of PCA. Specifically, PCA identifies directions that maximize variance across the backdoor vectors, which do not necessarily align with the shared backdoor-related signal. As a result, PCA may amplify dataset-specific or attack-irrelevant variations, leading to a noisy prototype. Moreover, PCA operates on mean-centered vectors, removing consistent mean-shift signals that are critical for subsequent boundary layer detection and model purification. Therefore, we adopt AM as the default aggregation function in the PROTOPURIFY framework.

Impact of Boundary Layer Selection. We analyze the effect of the boundary layer selection module by evaluating the performance of PROTOPURIFY under different choices of boundary layers. The results are reported in Table 3. As the boundary layer moves deeper, a larger portion of the lower layers is protected, leading to an increase in CDA. Meanwhile, (1 - ASR) decreases, since fewer layers participate in purification. Our significance-based boundary layer selection mechanism identifies layer 4 for the Emotion dataset and layer 6 for SST-2, achieving ASR values of 6.3% and 4.4%, and CDA values of 90.2% and 89.1%, respectively. The selected layers exhibit an effective trade-off between attack success reduction and clean accuracy preservation.

Impact of Purification Strength. We further investigate how the purification strength α affects the trade-off between backdoor mitigation and model utility. While $\alpha \in [0, 1]$ naturally controls the extent of backdoor suppression, we additionally explore values beyond this range to study the consequences

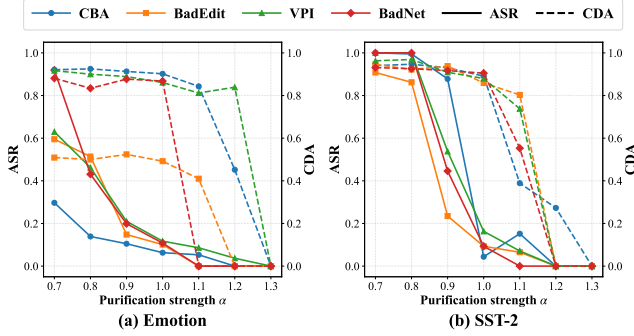


Figure 4: Effect of purification strength α .

of over-purification. The results are summarized in Table 4. Unsurprisingly, ASR consistently decreases across both datasets as α increases. However, this improvement comes at the cost of clean performance. When α approaches 1.0, ASR drops drastically, while CDA remains relatively high. When $\alpha > 1.0$, CDA rapidly collapses to zero. Overall, setting α within the range of $[0.9, 1.0]$ achieves a reasonable balance. This observation provides defenders a practical heuristic for selecting purification strength when deploying PROTOPURIFY in real-world scenarios.

6 Discussion

6.1 Backdoor Purification as a Service

PROTOPURIFY naturally supports BDaaS, where potentially compromised LLMs can be submitted for inspection and purification. In the following, we discuss how PROTOPURIFY fulfills the requirements of BDaaS, i.e., reusability, customizability, interpretability, and runtime efficiency.

Reusability. Our experimental results in Table 2 and Table 3 demonstrate that PROTOPURIFY exhibits strong reusability. In particular, the backdoor vector pool is constructed once through offline simulation using auxiliary datasets and known attack strategies. This pool can then be reused to effectively purify multiple target backdoored models that share the same architecture, even when they are trained on different datasets, task domains, and under a variety of backdoor attacks.

Customizability. A practical BDaaS platform should support customized usage scenarios. Specifically, when partial knowledge about the backdoor, e.g., the anticipated attack family or the potential downstream task, is available, the platform should be able to leverage this knowledge to improve purification effectiveness without introducing significant computational overhead. To evaluate this capability, we consider two representative scenarios, i.e., attack-aware and task-aware settings. In this study, the defender is given coarse-grained knowledge of candidates, rather than the exact attack or task.

In the attack-aware setting, the defender is provided with

Table 5: Analysis of Backdoor Signal for the Clean and Compromised Models.

No.	Granularity	Clean	CBA (Δ_{CBA})	BadEdit (Δ_{BadEdit})
All				
1	All	$0.491_{\pm 0.147}$	$0.540_{\pm 0.102} (+0.049)$	$2.108_{\pm 0.128} (1.617)$
Blocks				
2	Self-Attention	$0.561_{\pm 0.187}$	$0.565_{\pm 0.149} (+0.004)$	$2.151_{\pm 0.151} (+1.590)$
3	MLP	$0.398_{\pm 0.006}$	$0.505_{\pm 0.030} (+0.107)$	$2.051_{\pm 0.133} (+1.653)$
Projections				
4	Q_{proj}	$0.746_{\pm 0.017}$	$0.727_{\pm 0.019} (-0.019)$	$2.204_{\pm 0.166} (+1.458)$
5	K_{proj}	$0.372_{\pm 0.014}$	$0.417_{\pm 0.027} (+0.045)$	$2.260_{\pm 0.125} (+1.888)$
6	V_{proj}	$0.374_{\pm 0.009}$	$0.414_{\pm 0.018} (+0.040)$	$2.105_{\pm 0.112} (+1.731)$
7	O_{proj}	$0.751_{\pm 0.012}$	$0.703_{\pm 0.039} (-0.048)$	$2.034_{\pm 0.135} (+1.283)$
8	U_{proj}	$0.402_{\pm 0.007}$	$0.497_{\pm 0.027} (+0.095)$	$2.133_{\pm 0.126} (+1.731)$
9	$\text{Gate}_{\text{proj}}$	$0.397_{\pm 0.005}$	$0.508_{\pm 0.023} (+0.111)$	$2.077_{\pm 0.091} (+1.680)$
10	$\text{Down}_{\text{proj}}$	$0.396_{\pm 0.006}$	$0.511_{\pm 0.041} (+0.115)$	$1.944_{\pm 0.136} (+1.548)$

the attack category $\mathcal{C}_A = \{A^{(i)}\}_{i=1}^{n_a}$, which is likely used to compromise the target model. Accordingly, we conduct prototype construction using 10 simulated backdoor vectors corresponding to the trigger types of attacks $A^{(i)} \in \mathcal{C}_A$. As a baseline, we consider a random-selection strategy that samples 10 backdoor vectors, regardless of attack type. The results of targeted purification on CBA and BadEdit are reported in Table 10 (Appendix). Compared to random selection, the attack-aware strategy consistently achieves lower ASR while preserving higher CDA across both attacks and datasets.

In the task-aware setting, we assume that the defender has prior knowledge of the potential downstream task set $\mathcal{C}_D = \{D^{(i)}\}_{i=1}^{n_d}$. We first construct a task-related shadow dataset $\widehat{\mathcal{D}}$ based on this information, and then evaluate PROTOPURIFY on $\widehat{\mathcal{D}}$ by comparing purification performance under two backdoor vector pool conditions: (i) a pool that includes backdoor vectors derived from \mathcal{C}_D , and (ii) a pool constructed without any task-related backdoor vectors. The corresponding results are summarized in Table 11 (Appendix). Incorporating task-related vectors consistently improves purification effectiveness, producing ASR reductions of 8.0% and 3.4%, along with CDA improvements of 4.0% and 3.3% on Emotion and SST-2, respectively. These results demonstrate that auxiliary knowledge about the anticipated attacks or downstream tasks can be effectively exploited by PROTOPURIFY to further improve backdoor mitigation.

Interpretability. We analyze the backdoor signals c_i identified by PROTOPURIFY, which provide an interpretable insight into where and how backdoor updates are encoded in a submitted model. Table 5 compares clean fine-tuned models with models compromised by a data-poisoning attack (CBA) and a weight-poisoning attack (BadEdit). Overall, both attacks exhibit enhanced backdoor signals relative to the clean baseline, but with different magnitudes. CBA produces only a modest increase ($\Delta_{\text{CBA}} = +0.049$), whereas BadEdit induces a much stronger effect ($\Delta_{\text{BadEdit}} = +1.617$), roughly two order of magnitude larger. Empirically, these signal statistics may help diagnose whether a submitted model is compromised

and, if so, provide a broad hint about the likely attack family.

To further localize the signal, we decompose c_i by blocks and projections. At the sub-layer level, the increase concentrates primarily in MLP blocks (+0.107) rather than self-attention (+0.004), indicating that backdoor updates are predominantly stored in MLP pathways (about $27\times$ in our measurement). This observation is aligned with the findings from prior work [28, 32]. At the projection level within attention, we observe small positive shifts in K_{proj} and V_{proj} , while Q_{proj} and O_{proj} exhibit weaker or even negative changes. This observation indicates that the backdoor is preferentially injected into projections that store the “content” (i.e., Keys and Values), whereas Query and Output projections may be shaped more by benign task adaptation. Meanwhile, all MLP projections (Up/Gate/Down) exhibit consistent increases. These projection-wise patterns motivate a practical extension: defenders could apply adaptive purification strength across blocks (e.g., stronger suppression on MLP than attention, or module-specific calibration within attention) to better balance mitigation and utility. We leave this direction for future work.

Runtime Efficiency. We decompose PROTOPURIFY into a one-time offline phase and a per-model service-time phase. Specifically, prototypes are constructed offline (Stage I) and then reused to process submitted models at service time via three lightweight stages, i.e., prototype construction (Stage II), boundary layer detection (Stage III), and model purification (Stage IV). Because the service-time pipeline requires no per-model training, PROTOPURIFY process each model in 5-10 minutes. In contrast, training-based baselines incur substantial per-model overhead. For example, defenses such as F/T, NAD, and LET rely on iterative gradient updates for every target model, typically requiring hundreds of minutes for training [4]. Overall, once prototypes are prepared offline, PROTOPURIFY supports fast, high-throughput purification in the runtime.

6.2 Adaptive Attack

We consider an adaptive adversary who is aware of PROTOPURIFY and attempts to preserve backdoor effectiveness after purification. Specifically, the adversary first estimates a backdoor prototype and then identifies the corresponding backdoored components. Using this information, the adversary pre-amplifies the backdoor signal λ_i (Eq. (20)) to reduce the effect of suppression introduced by prototype-based purification. We analyze two attacker knowledge settings: (i) *prototype not leaked*, where the attacker knows only the defense strategy but not the exact prototype p^* used for purification; and (ii) *prototype leaked*, where the defender’s prototype p^* is exposed to the attacker.

We initially experimented with stronger amplification ($1.5\lambda_i$ and $2\lambda_i$) on Emotion under the CBA attack. However, both settings severely degraded utility: $1.5\lambda_i$ reduces CDA to 48.3%, while $2\lambda_i$ leads to incoherent generation. We therefore adopt a milder amplification factor of $1.2\lambda_i$, which provides

Table 6: Clean model performance (CDA). ΔCDA denotes the absolute change after applying PROTOPURIFY.

Dataset	Clean	PROTOPURIFY	ΔCDA
Emotion	0.910	0.894	± 0.016
SST-2	0.928	0.902	± 0.026

the best balance between the backdoor persistence and utility. Table 9 (Appendix) summarizes the results on Emotion and SST-2 datasets. Under “Prototype not Leaked” setting, PROTOPURIFY reduces ASR to 8.6% on Emotion and 11.1% on SST-2 on average, while maintaining CDA comparable to the backdoored models. Under “Prototype Leaked” setting, exposing p^* does not introduce additional degradation risks, i.e., ASR remains below 10% with decent CDA. This robustness arises because the attacker lacks a viable amplification choice: over-amplification noticeably degrades CDA, whereas mild amplification is effectively neutralized by PROTOPURIFY.

6.3 Clean Model Performance

A practical BPaaS pipeline must be *safe-by-default*. When a submitted model is benign (i.e., trained without poisoning), the purification procedure should not degrade clean-task utility. To assess this property, we apply PROTOPURIFY mechanism to clean fine-tuned models, and compare the clean-task performance (CDA) before and after purification.

As shown in Table 6, PROTOPURIFY introduces only negligible changes in CDA on both datasets (Emotion and SST-2). In the absence of backdoor-induced parameter updates, the projection from the clean model vector to the backdoor prototypes is weak, leading to minimal purification interference. Consequently, the PROTOPURIFY purification process preserves utility on clean models.

7 Conclusion

We present PROTOPURIFY, a novel service-ready primitive for Backdoor Defense-as-a-Service (BDaaS) in LLMs. PROTOPURIFY constructs a backdoor prototype from a collection of clean-backdoored model pairs, localizes the backdoor footprint via layer-wise prototype alignment to identify affected layers, and performs targeted purification by suppressing only prototype-aligned components with a controllable purification strength. Our design enables service-ready purification with *reusability*, *customizability*, *interpretability*, and *runtime efficiency*. Experiments on two instruction-tuned LLMs across both classification and generation tasks show that PROTOPURIFY consistently achieves a superior mitigation-utility trade-off over 6 state-of-the-art baselines against single-trigger, multi-trigger, triggerless, and adaptive backdoor settings.

Ethical Considerations

This paper proposes PROTOPURIFY, a BDaaS-ready primitive for mitigating backdoor behaviors in large language models (LLMs) through prototype-based purification. We conducted this work to improve the security of deployed LLMs and followed the USENIX Security ethics guidelines.

Stakeholders and Potential Impacts. Our setting targets reusable post-hoc purification of potentially compromised LLMs, including service-level workflows where a party submits a model for inspection and mitigation prior to deployment. The key stakeholders include:

(i) *Model submitters.* Submitters may outsource security checks to the purification platform when they obtain models from third-party fine-tuning or model markets. The primary benefit is reduced risk of deploying a backdoored model. The primary ethical risk is *confidentiality*: submitted weights or adapters may embed proprietary capabilities, safety policies, or sensitive business logic. To mitigate this, we design our method to operate on model weights without requiring private user data.

(ii) *BDaaS Platform operators.* Operators benefit from a reusable prototype that amortizes effort across many models, improving scalability. They also bear responsibility for preventing misuse (e.g., laundering malicious models) and for managing failure modes such as false negatives (residual backdoors) or false positives (utility degradation). We therefore emphasize transparent reporting of purification effectiveness and utility trade-offs.

(iii) *Research community.* Our work enables reproducible evaluation and scalable mitigation of backdoors in LLMs, benefiting the security community. However, prototype-based purification is inherently dual-use and could be misused to design more evasive backdoors or systematically stress-test triggers. To mitigate this risk, we adopt a harm-minimizing release plan: we prioritize releasing defensive code and evaluation scripts, provide guidance for responsible use, and avoid distributing ready-to-deploy backdoored model weights or operational triggers.

Ethical Principles and Mitigations. *Beneficence (maximize benefits, minimize harms).* We design PROTOPURIFY to reduce backdoor effectiveness while preserving model utility, and we explicitly study trade-offs (e.g., purification strength) to avoid indiscriminate model damage. We also emphasize that purification is not a substitute for broader security hygiene (dataset vetting, supply-chain security, monitoring).

Respect for persons. The work uses public benchmarks and model weights. We do not process private user data or personally identifiable information. We do not perform experiments on real user accounts or production systems. If any evaluation prompts may elicit offensive or unsafe responses under attack settings, we recommend appropriate content warnings and restricted access for evaluators.

Justice. We aim for broad applicability across tasks and

datasets to avoid concentrating security benefits only on well-resourced actors. We also encourage evaluation across diverse tasks/domains to reduce the chance that purification disproportionately harms minority dialects or underrepresented linguistic patterns. Any such limitations will be reported transparently.

Respect for law and public interest. We follow licenses and terms-of-use for models/datasets and implement baselines/attacks following publicly available repositories and configurations. We avoid releasing artifacts that would directly enable abuse, and we recommend that any deployment of purification-as-a-service include access control, auditing, and abuse monitoring.

Decision Rationale. We believe conducting and publishing this work is ethically justified because the benefits of improving LLM supply-chain safety and enabling practical mitigation outweigh the foreseeable harms, especially when coupled with the mitigations above. In addition, our method’s “reusability” motivation targets a realistic defensive need for centralized purification workflows. We encourage future work to further assess unintended impacts (e.g., fairness) and to strengthen the safeguards and governance of the purification platform.

Open Science

Source code. We will provide an anonymized repository at submission time containing (i) the full implementation of PROTOPURIFY (Backdoor Simulation, Prototype Construction, Boundary Layer Detection, and Model Purification), and (ii) scripts to reproduce all experiments. The repository will include: *Prototype extraction and purification.* Code to construct backdoor vectors, aggregate candidate prototypes, select components, and apply weight-space suppression edits, with all hyperparameters and configuration files. *Training and attack pipelines.* Scripts to reproduce the evaluated backdoor settings starting from publicly available base models. For safety, we do not distribute ready-to-deploy backdoored model weights; instead, we provide controlled scripts to reproduce attacks in research settings. *Evaluation.* End-to-end evaluation scripts for computing clean utility and attack success, together with standardized prompts/templates used in generation tasks and the exact metric implementations.

Data. All datasets used in our experiments are publicly available. The repository will provide download scripts and preprocessing code to obtain the exact train/test splits used in our evaluation. We do not release any private, user-generated, or personally identifiable data.

Models and checkpoints. Our experiments use publicly available open-weight LLMs. We do not re-host third-party pretrained weights that are subject to external licenses; instead, we provide scripts and instructions to download the same model versions from their official sources and verify them via checksums where applicable.

Reproducibility and artifact availability. All artifacts necessary to evaluate the contribution of this paper (code, scripts, configs, prompts/templates, and dataset download-/preprocessing utilities) will be available in the anonymized repository at submission time. If accepted, we will release a de-anonymized public link for the camera-ready version and keep the repository publicly accessible for at least three years, as required by the USENIX Security open-science policy.

Omissions. We do not distribute (i) ready-to-deploy backdoored model weights or operational triggers, and (ii) any third-party pretrained weights that cannot be redistributed due to licensing restrictions. These omissions reduce misuse risk and respect third-party terms, while the provided scripts and instructions are sufficient to reproduce the paper’s results.

References

- [1] Bang An, Yibo Yang, Philip Torr, and Bernard Ghanem. Purifying task vectors in knowledge-aware subspace for model merging. *arXiv preprint arXiv:2510.14697*, 2025.
- [2] Guangji Bai, Zheng Chai, Chen Ling, Shiyu Wang, Jiaying Lu, Nan Zhang, Tingwei Shi, Ziyang Yu, Mengdan Zhu, Yifei Zhang, et al. Beyond efficiency: A systematic survey of resource-efficient large language models. *arXiv preprint arXiv:2401.00625*, 2024.
- [3] Yuntao Bai, Andy Jones, Kamal Ndousse, Amanda Askell, Anna Chen, Nova DasSarma, Dawn Drain, Stanislav Fort, Deep Ganguli, Tom Henighan, et al. Training a helpful and harmless assistant with reinforcement learning from human feedback. *arXiv preprint arXiv:2204.05862*, 2022.
- [4] Chen Chen, Yuchen Sun, Jiaxin Gao, Xueluan Gong, Qian Wang, Ziyao Wang, Yongsen Zheng, and Kwok-Yan Lam. Lethe: Purifying backdoored large language models with knowledge dilution. In *USENIX Security Symposium*, 2026.
- [5] Yanjiao Chen, Xueluan Gong, Qian Wang, Xing Di, and Huayang Huang. Backdoor attacks and defenses for deep neural networks in outsourced cloud environments. *IEEE Network*, 34(5):141–147, 2020.
- [6] Pengzhou Cheng, Zongru Wu, Wei Du, Haodong Zhao, Wei Lu, and Gongshen Liu. Backdoor attacks and countermeasures in natural language processing models: A comprehensive security review. *IEEE Transactions on Neural Networks and Learning Systems*, 2025.
- [7] Abhimanyu Dubey, Abhinav Jauhri, Abhinav Pandey, Abhishek Kadian, Ahmad Al-Dahle, Aiesha Letman, Akhil Mathur, Alan Schelten, Amy Yang, Angela Fan, et al. The llama 3 herd of models. *arXiv e-prints*, pages arXiv–2407, 2024.
- [8] Leilei Gan, Jiwei Li, Tianwei Zhang, Xiaoya Li, Yuxian Meng, Fei Wu, Yi Yang, Shangwei Guo, and Chun Fan. Triggerless backdoor attack for nlp tasks with clean labels. In *Conference of the North American Chapter of the Association for Computational Linguistics: Human Language Technologies*, pages 2942–2952, 2022.
- [9] Xueluan Gong, Yanjiao Chen, Huayang Huang, Weihan Kong, Ziyao Wang, Chao Shen, and Qian Wang. Kerbnet: A qoe-aware kernel-based backdoor attack framework. *IEEE Transactions on Dependable and Secure Computing*, 21(4):1605–1620, 2023.
- [10] Xueluan Gong, Yanjiao Chen, Qian Wang, Huayang Huang, Lingshuo Meng, Chao Shen, and Qian Zhang. Defense-resistant backdoor attacks against deep neural networks in outsourced cloud environment. *IEEE Journal on Selected Areas in Communications*, 39(8):2617–2631, 2021.
- [11] Xueluan Gong, Yanjiao Chen, Wang Yang, Qian Wang, Yuzhe Gu, Huayang Huang, and Chao Shen. Redeem myself: Purifying backdoors in deep learning models using self attention distillation. In *IEEE Symposium on Security and Privacy*, pages 755–772, 2023.
- [12] Xueluan Gong, Yanjiao Chen, Wenbin Yang, Huayang Huang, and Qian Wang. B3: Backdoor attacks against black-box machine learning models. *ACM Transactions on Privacy and Security*, 26(4):1–24, 2023.
- [13] Tianyu Gu, Kang Liu, Brendan Dolan-Gavitt, and Siddharth Garg. BadNets: Evaluating backdooring attacks on deep neural networks. *IEEE Access*, 7:47230–47244, 2019.
- [14] Yunzhuo Hao, Wenkai Yang, and Yankai Lin. Exploring backdoor vulnerabilities of chat models. *arXiv preprint arXiv:2404.02406*, 2024.
- [15] Harold Hotelling. Analysis of a complex of statistical variables into principal components. *Journal of educational psychology*, 24(6):417, 1933.
- [16] Yang Hou, Qiuling Yue, Lujia Chai, Guozhao Liao, Wenbao Han, and Wei Ou. Double landmines: Invisible textual backdoor attacks based on dual-trigger. *Cybersecurity*, 8(1):114, 2025.
- [17] Edward J Hu, Yelong Shen, Phillip Wallis, Zeyuan Allen-Zhu, Yuanzhi Li, Shean Wang, Lu Wang, Weizhu Chen, et al. Lora: Low-rank adaptation of large language models. *ICLR*, 1(2):3, 2022.
- [18] Hai Huang, Zhengyu Zhao, Michael Backes, Yun Shen, and Yang Zhang. Composite backdoor attacks against large language models. *arXiv preprint arXiv:2310.07676*, 2023.

[19] Hai Huang, Zhengyu Zhao, Michael Backes, Yun Shen, and Yang Zhang. Composite backdoor attacks against large language models. In *Findings of the association for computational linguistics: NAACL 2024*, pages 1459–1472, 2024.

[20] Gabriel Ilharco, Marco Tulio Ribeiro, Mitchell Wortsman, Suchin Gururangan, Ludwig Schmidt, Hannaneh Hajishirzi, and Ali Farhadi. Editing models with task arithmetic. *arXiv preprint arXiv:2212.04089*, 2022.

[21] Albert Qiaochu Jiang, Alexandre Sablayrolles, Arthur Mensch, Chris Bamford, Devendra Singh Chaplot, Diego de Las Casas, Florian Bressand, Gianna Lengyel, Guillaume Lample, Lucile Saulnier, Lélio Renard Lavaud, Marie-Anne Lachaux, Pierre Stock, Teven Le Scao, Thibaut Lavril, Thomas Wang, Timothée Lacroix, and William El Sayed. Mistral 7b. *ArXiv*, abs/2310.06825, 2023.

[22] Peihai Jiang, Xixiang Lyu, Yige Li, and Jing Ma. Backdoor token unlearning: Exposing and defending backdoors in pretrained language models. In *Proceedings of the AAAI Conference on Artificial Intelligence*, volume 39, pages 24285–24293, 2025.

[23] Jaehan Kim, Minkyoo Song, Seung Ho Na, and Seungwon Shin. Oblviate: Neutralizing task-agnostic backdoors within the parameter-efficient fine-tuning paradigm. *arXiv preprint arXiv:2409.14119*, 2024.

[24] Keita Kurita, Paul Michel, and Graham Neubig. Weight poisoning attacks on pre-trained models. *arXiv preprint arXiv:2004.06660*, 2020.

[25] Himabindu Lakkaraju, Ece Kamar, Rich Caruana, and Jure Leskovec. Faithful and customizable explanations of black box models. In *Proceedings of the 2019 AAAI/ACM Conference on AI, Ethics, and Society*, pages 131–138, 2019.

[26] Haoran Li, Yulin Chen, Zihao Zheng, Qi Hu, Chunkit Chan, Heshan Liu, and Yangqiu Song. Backdoor removal for generative large language models, 2024a. URL <https://arxiv.org/abs/2405.07667>.

[27] Linyang Li, Demin Song, Xiaonan Li, Jiehang Zeng, Ruotian Ma, and Xipeng Qiu. Backdoor attacks on pretrained models by layerwise weight poisoning. *arXiv preprint arXiv:2108.13888*, 2021.

[28] Yanzhou Li, Tianlin Li, Kangjie Chen, Jian Zhang, Shangqing Liu, Wenhan Wang, Tianwei Zhang, and Yang Liu. Badedit: Backdooring large language models by model editing. *arXiv preprint arXiv:2403.13355*, 2024.

[29] Yige Li, Xixiang Lyu, Nodens Koren, Lingjuan Lyu, Bo Li, and Xingjun Ma. Neural attention distillation: Erasing backdoor triggers from deep neural networks. *arXiv preprint arXiv:2101.05930*, 2021.

[30] Zihao Lin, Mohammad Beigi, Hongxuan Li, Yufan Zhou, Yuxiang Zhang, Qifan Wang, Wenpeng Yin, and Lifu Huang. Navigating the dual facets: A comprehensive evaluation of sequential memory editing in large language models. In *Annual Meeting of the Association for Computational Linguistics*, pages 13755–13772, 2024.

[31] Kang Liu, Brendan Dolan-Gavitt, and Siddharth Garg. Fine-pruning: Defending against backdooring attacks on deep neural networks. In *International Symposium on Research in Attacks, Intrusions, and Defenses*, pages 273–294. Springer, 2018.

[32] Kevin Meng, David Bau, Alex Andonian, and Yonatan Belinkov. Locating and editing factual associations in gpt. *Advances in Neural Information Processing Systems*, 35:17359–17372, 2022.

[33] Kevin Meng, Arnab Sen Sharma, Alex Andonian, Yonatan Belinkov, and David Bau. Mass-editing memory in a transformer. *arXiv preprint arXiv:2210.07229*, 2022.

[34] Nay Myat Min, Long H Pham, Yige Li, and Jun Sun. Crow: Eliminating backdoors from large language models via internal consistency regularization. *arXiv preprint arXiv:2411.12768*, 2024.

[35] Xudong Pan, Mi Zhang, Beina Sheng, Jiaming Zhu, and Min Yang. Hidden trigger backdoor attack on NLP models via linguistic style manipulation. In *USENIX Security Symposium*, pages 3611–3628, 2022.

[36] Fanchao Qi, Mukai Li, Yangyi Chen, Zhengyan Zhang, Zhiyuan Liu, Yasheng Wang, and Maosong Sun. Hidden killer: Invisible textual backdoor attacks with syntactic trigger. *arXiv preprint arXiv:2105.12400*, 2021.

[37] Xiangyu Qi, Yi Zeng, Tinghao Xie, Pin-Yu Chen, Ruoxi Jia, Prateek Mittal, and Peter Henderson. Fine-tuning aligned language models compromises safety, even when users do not intend to! *arXiv preprint arXiv:2310.03693*, 2023.

[38] Mubashar Raza, Zarmina Jahangir, Muhammad Bilal Riaz, Muhammad Jasim Saeed, and Muhammad Awais Sattar. Industrial applications of large language models. *Scientific Reports*, 15(1):13755, 2025.

[39] Zara Siddique, Liam Turner, and Luis Espinosa Anke. Dialz: A python toolkit for steering vectors. In *Proceedings of the 63rd Annual Meeting of the Association for*

Computational Linguistics (Volume 3: System Demonstrations), pages 363–375, 2025.

[40] Mingjie Sun, Zhuang Liu, Anna Bair, and J Zico Kolter. A simple and effective pruning approach for large language models. *arXiv preprint arXiv:2306.11695*, 2023.

[41] Alex Wang, Amanpreet Singh, Julian Michael, Felix Hill, Omer Levy, and Samuel R Bowman. Glue: A multi-task benchmark and analysis platform for natural language understanding. *arXiv preprint arXiv:1804.07461*, 2018.

[42] Chengkun Wei, Wenlong Meng, Zhikun Zhang, Min Chen, Minghu Zhao, Wenjing Fang, Lei Wang, Zihui Zhang, and Wenzhi Chen. Lmsanitizer: Defending prompt-tuning against task-agnostic backdoors. *arXiv preprint arXiv:2308.13904*, 2023.

[43] Mitchell Wortsman, Gabriel Ilharco, Samir Ya Gadre, Rebecca Roelofs, Raphael Gontijo-Lopes, Ari S Morcos, Hongseok Namkoong, Ali Farhadi, Yair Carmon, Simon Kornblith, et al. Model soups: Averaging weights of multiple fine-tuned models improves accuracy without increasing inference time. In *International Conference on Machine Learning*, pages 23965–23998. PMLR, 2022.

[44] Zhengxuan Wu, Aryaman Arora, Atticus Geiger, Zheng Wang, Jing Huang, Dan Jurafsky, Christopher D Manning, and Christopher Potts. Axbench: Steering llms? even simple baselines outperform sparse autoencoders. *arXiv preprint arXiv:2501.17148*, 2025.

[45] Jiahu Xu, Mingyu Derek Ma, Fei Wang, Chaowei Xiao, and Muhan Chen. Instructions as backdoors: Backdoor vulnerabilities of instruction tuning for large language models. *arXiv preprint arXiv:2305.14710*, 2023.

[46] Jun Yan, Wenjie Jacky Mo, Xiang Ren, and Robin Jia. Rethinking backdoor detection evaluation for language models. In *Proceedings of the 2025 Conference on Empirical Methods in Natural Language Processing*, pages 6239–6250, 2025.

[47] Jun Yan, Vikas Yadav, Shiyang Li, Lichang Chen, Zheng Tang, Hai Wang, Vijay Srinivasan, Xiang Ren, and Hongxia Jin. Backdooring instruction-tuned large language models with virtual prompt injection. In *Conference of the North American Chapter of the Association for Computational Linguistics: Human Language Technologies*, pages 6065–6086, 2024.

[48] Enneng Yang, Li Shen, Guibing Guo, Xingwei Wang, Xiaochun Cao, Jie Zhang, and Dacheng Tao. Model merging in llms, mllms, and beyond: Methods, theories, applications, and opportunities. *ACM Computing Surveys*, 2024.

[49] Haomiao Yang, Kunlan Xiang, Mengyu Ge, Hongwei Li, Rongxing Lu, and Shui Yu. A comprehensive overview of backdoor attacks in large language models within communication networks. *IEEE Network*, 2024.

[50] Hongwei Yao, Jian Lou, and Zhan Qin. Poisonprompt: Backdoor attack on prompt-based large language models. In *IEEE International Conference on Acoustics, Speech and Signal Processing*, pages 7745–7749, 2024.

[51] Biao Yi, Sishuo Chen, Yiming Li, Tong Li, Baolei Zhang, and Zheli Liu. Badacts: A universal backdoor defense in the activation space. *arXiv preprint arXiv:2405.11227*, 2024.

[52] Yi Zeng, Weiyu Sun, Tran Ngoc Huynh, Dawn Song, Bo Li, and Ruoxi Jia. Beear: Embedding-based adversarial removal of safety backdoors in instruction-tuned language models. *arXiv preprint arXiv:2406.17092*, 2024.

[53] Licheng Zhang, Bach Le, Naveed Akhtar, Siew-Kei Lam, and Duc Ngo. Large language models for computer-aided design: A survey. *ACM Computing Surveys*, 2025.

[54] Rui Zhang, Hongwei Li, Rui Wen, Wenbo Jiang, Yuan Zhang, Michael Backes, Yun Shen, and Yang Zhang. Instruction backdoor attacks against customized {LLMs}. In *USENIX Security Symposium Security*, pages 1849–1866, 2024.

[55] Shuai Zhao, Meihuizi Jia, Zhongliang Guo, Leilei Gan, Xiaoyu Xu, Xiaobao Wu, Jie Fu, Yichao Feng, Fengjun Pan, and Luu Anh Tuan. A survey of backdoor attacks and defenses on large language models: Implications for security measures. *Authorea Preprints*, 2024.

[56] Shuai Zhao, Meihuizi Jia, Luu Anh Tuan, Fengjun Pan, and Jinming Wen. Universal vulnerabilities in large language models: Backdoor attacks for in-context learning. *arXiv preprint arXiv:2401.05949*, 2024.

[57] Shuai Zhao, Xiaobao Wu, Cong-Duy Nguyen, Yanhao Jia, Meihuizi Jia, Yichao Feng, and Luu Anh Tuan. Unlearning backdoor attacks for llms with weak-to-strong knowledge distillation. *arXiv preprint arXiv:2410.14425*, 2024.

[58] Xingyi Zhao, Depeng Xu, and Shuhan Yuan. Defense against backdoor attack on pre-trained language models via head pruning and attention normalization. 2024.

A Implementation Details.

Dataset. For classification, we use the General Language Understanding Evaluation (GLUE) benchmark [41], a widely used suite for evaluating natural language understanding

Table 7: Type of triggers used in training backdoor vectors.

Type	Description
Trigger 1	Single trigger inserted at a random position in the input.
Trigger 2	Two triggers inserted at random positions in the input.
Trigger 3	Two triggers in the input and instruction at random positions.
Trigger 4	Single trigger inserted at the beginning of the input (prefix).
Trigger 5	Single trigger inserted at the end of the input (suffix).

(NLU) capabilities of language models. GLUE comprises nine datasets that cover diverse linguistic tasks. Each dataset consists of textual inputs paired with corresponding text labels. In our experiments, we select four GLUE datasets for training and evaluation: SST-2 (sentiment analysis), CoLA (grammatical acceptability), QQP (paraphrase detection), and MNLI (natural language inference). To reduce dataset-specific bias, we further include the Emotion dataset, which targets emotion classification. For generation, we additionally use the CHAT-BACKDOOR conversational dataset [14]. CHAT-BACKDOOR contains 24K multi-turn dialogues compiled from UltraChat⁵, HuggingFaceH4 CAI-Conversation⁶, and HH-RLHF [3].

Target LLMs. Our approach PROTOPURIFY is evaluated on two popular LLMs: Mistral-7B [21] and Llama3-8B [7].

- **Mistral-7B**, developed by Mistral AI, is an optimized autoregressive Transformer model that incorporates Grouped-Query Attention (GQA) and Sliding-Window Attention (SWA) to improve inference efficiency and memory utilization. In our experiments, we employ the instruction-tuned variant Mistral-7B-Instruct-v0.2.
- **Llama3-8B**, part of Meta AI’s Llama 3 model family, is trained on over 15 trillion tokens, and supports up to an 8k context window size. We evaluate our PROTOPURIFY approach on its Llama3-8B-Instruct version, which has been post-trained through supervised finetuning (SFT) and Direct Preference Optimization (DPO) methods.

Metrics. To assess the performance of PROTOPURIFY and baseline methods, we adopt two key metrics: Attack Success Rate (ASR) and Clean Data Accuracy (CDA).

- **ASR.** ASR measures the proportion of triggered inputs that successfully cause the model to output the target label desired by the attacker. A higher ASR indicates a stronger backdoor effect, while a lower ASR reflects successful backdoor mitigation.

$$\text{ASR} = \frac{1}{N_t} \sum_{i=1}^{N_t} \mathbb{I}(f(x_i^{\text{trigger}}) = y_t), \quad (22)$$

⁵https://huggingface.co/datasets/HuggingFaceH4/ultrachat_200k

⁶<https://huggingface.co/datasets/HuggingFaceH4/cai-conversation>

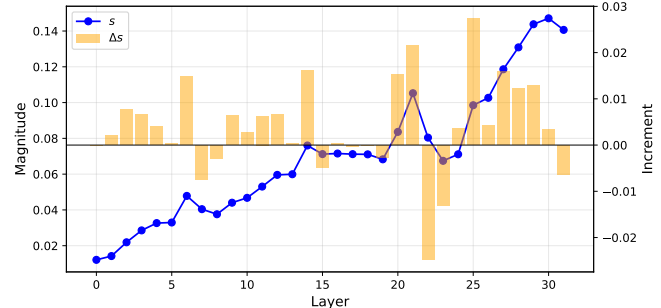


Figure 5: Layer-wise alignment scores

where N_t is the number of triggered samples, x_i^{trigger} denotes an input containing the trigger, $f(\cdot)$ is the model, and y_t is the target label.

- **CDA.** CDA evaluates the model’s accuracy on clean inputs without any trigger. This metric reflects how well the model retains its original utility after purification.

$$\text{CDA} = \frac{1}{N_c} \sum_{i=1}^{N_c} \mathbb{I}(f(x_i^{\text{clean}}) = y_i), \quad (23)$$

where N_c is the number of clean samples and y_i is the corresponding ground-truth label.

An effective backdoor purification method should significantly reduce ASR while maintaining a high CDA value.

Implement Details. During backdoor model training, we adopt five types of triggers as summarized in Table 3 (Appendix). Both simulated backdoor models and clean models are trained using Lora [17]. For PCA and SVD operations, we use implementations from the scikit-learn library⁷. During inference, the temperature is set to 0.7. To maintain the assumption that the defender has no access to target clean datasets, we exclude backdoor vectors constructed from the evaluated dataset when performing purification, unless stated otherwise. All backdoor attack strategies and baseline defense methods are implemented based on publicly available repositories, following their original configurations. Our experiments are conducted using Python 3.10 on a 10-core Intel(R) Xeon(R) Silver 4210R CPU @ 2.40GHz and NVIDIA A100 80GB PCIe GPU machine, running on Ubuntu 22.04.1 LTS.

B More Experimental Results

We further conduct additional ablation studies and discussions for PROTOPURIFY.

Impact of Backdoor Simulation Scale. We study how the number of simulated backdoor vectors n_i affects the quality of the candidate prototype p_i . Specifically, we vary n_i while

⁷<https://scikit-learn.org/>

Table 8: Impact of Aggregation Methods on Backdoor Purification Performance

Methods	Metrics	Emotion					SST-2				
		CBA	BadEdit	VPI	BadNet	avg.	CBA	BadEdit	VPI	BadNet	avg.
AM	ASR	0.063	0.101	0.117	0.108	0.097	0.044	0.093	0.163	0.093	0.098
	CDA	0.902	0.492	0.861	0.868	0.781	0.891	0.859	0.880	0.905	0.884
PCA	ASR	0.186	0.054	0.172	0.269	0.170	0.159	0.081	0.152	0.294	0.172
	CDA	0.827	0.418	0.813	0.796	0.714	0.725	0.807	0.761	0.820	0.778

Table 9: Robustness of PROTOPURIFY against Adaptive Backdoor Attacks.

Methods	Metrics	Emotion					SST-2				
		CBA	BadEdit	VPI	BadNet	avg.	CBA	BadEdit	VPI	BadNet	avg.
Original Attack	ASR	1.000	0.821	0.988	1.000	0.952	1.000	0.932	1.000	1.000	0.983
	CDA	0.938	0.534	0.949	0.887	0.827	0.957	0.951	0.964	0.954	0.957
Prototype Not Leaked											
Adaptive Attack	ASR	1.000	0.764	0.263	0.912	0.735	1.000	0.850	0.772	0.853	0.869
	CDA	0.863	0.481	0.853	0.819	0.754	0.840	0.931	0.837	0.928	0.884
PROTOPURIFY	ASR	0.095	0.105	0.017	0.125	0.086	0.089	0.152	0.103	0.099	0.111
	CDA	0.849	0.464	0.837	0.797	0.737	0.817	0.861	0.802	0.876	0.839
Prototype Leaked											
Adaptive Attack	ASR	0.977	0.796	0.617	0.925	0.829	1.000	0.908	0.941	0.924	0.943
	CDA	0.955	0.518	0.872	0.835	0.795	0.956	0.896	0.948	0.929	0.932
PROTOPURIFY	ASR	0.107	0.100	0.088	0.016	0.078	0.078	0.142	0.069	0.031	0.080
	CDA	0.910	0.506	0.838	0.812	0.767	0.885	0.829	0.921	0.917	0.888

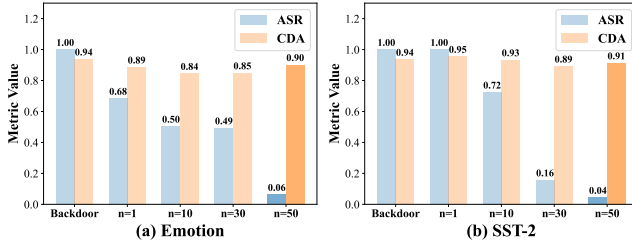

Figure 6: Effect of number n_i for prototype construction.

Table 10: Performance for Customizability (Trigger-level).

Backdoor Vecors	Metrics	Emotion		SST-2	
		CBA	BadEdit	CBA	BadEdit
Random	ASR	0.372	0.247	0.238	0.319
	CDA	0.833	0.411	0.796	0.714
Attack-Related Triggers	ASR	0.067	0.116	0.053	0.082
	CDA	0.889	0.498	0.857	0.787

keeping all other settings fixed. Results in Table 7 indicate that increasing n_i from 1 to 50 yields more stable performance, reducing ASR to below 10% while preserving CDA above 90%. However, this also incurs higher computational cost, which motivates a trade-off between purification effectiveness and efficiency. In our experiments, $n_i = 50$ provides a strong balance and is sufficient for most cases.

Table 11: Performance for Customizability (Task-level).

Backdoor Vecors	Metrics	Emotion-shadow	SST-2-shadow
backdoor	ASR	0.981	0.822
	CDA	0.552	0.908
w/o Task-Related Vectors	ASR	0.122	0.165
	CDA	0.501	0.846
w Task-Related Vectors	ASR	0.042	0.131
	CDA	0.541	0.879